AIMS Mathematics, 10(1): 234–269.
DOI: 10.3934/math.2025012
Received: 26 August 2024
Revised: 10 December 2024
Accepted: 24 December 2024
Published: 03 January 2025

http://www.aimspress.com/journal/Math

Research article

Exploring fractional Advection-Dispersion equations with computational methods: Caputo operator and Mohand techniques

Azzh Saad Alshehry[1], **Humaira Yasmin**[2,3,*] **and Ali M. Mahnashi**[4]

[1] Department of Mathematical Sciences, Faculty of Sciences, Princess Nourah Bint Abdulrahman University, P.O.Box 84428, Riyadh 11671, Saudi Arabia

[2] Department of Basic Sciences, General Administration of Preparatory Year, King Faisal University, P.O. Box 400, Al Ahsa 31982, Saudi Arabia

[3] Department of Mathematics and Statistics, College of Science, King Faisal University, P.O. Box 400, Al Ahsa 31982, Saudi Arabia

[4] Department of Mathematics, Faculty of Science, Jazan University, P.O. Box 2097, Jazan 45142, Kingdom of Saudi Arabia

* **Correspondence:** Email: hhassain@kfu.edu.sa.

Abstract: This study presented a comprehensive analysis of nonlinear fractional systems governed by the advection-dispersion equations (ADE), utilizing the Mohand transform iterative method (MTIM) and the Mohand residual power series method (MRPSM). By incorporating the Caputo fractional derivative, we enhanced the modeling capability for fractional-order differential equations, accounting for nonlocal effects and memory in the systems dynamics. We demonstrated that both MTIM and MRPSM were effective for solving fractional ADEs, providing accurate numerical solutions that were validated against exact results. The steady-state solutions, complemented by graphical representations, highlighted the behavior of the system for varying fractional orders and showcased the flexibility and robustness of the methods. These findings contributed significantly to the field of computational physics, offering powerful tools for tackling complex fractional-order systems and advancing research in related fields.

Keywords: Advection-Dispersion equations (ADE); Mohand transform iterative method (MTIM); Mohand residual power series method (MRPSM); fractional order differential equation; Caputo operator

Mathematics Subject Classification: 34G20, 35A20, 35A22, 35R11

1. Introduction

Many kinds of mathematical models have been developed to assist in the realization of some known physical phenomena. The derivatives of unknown functions are involved in these models, even though they yield differential equations (DEs). Since their development, the DEs have become an essential area of mathematics [1]. Soon after the Newtonian variable equations were developed in the 1670s, Leibniz and the Bernoulli brothers started working on DEs in the early 1680s. As a result, several writers created a variety of applications in engineering and mechanical subjects, which in turn enhanced the Leibnizian legacy and increased its multivariate form in the modern era [1]. Despite being more broad than ordinary differential equations (ODEs), partial differential equations (PDEs) typically require a distinct approach to be solved [2–4]. They encompass solving problems involving several independent variables, making them more difficult and complex even when the subject matter is vast and important. In fact, PDE solutions have drawn a lot of attention from scientists since certain phenomena have found a way to be expressed through them [5]. The two most well-known examples of linear PDEs are heat and wave equations, whereas the most well-known examples of nonlinear PDEs include Schrodinger, Poisson, Korteweg-de Vries, water wave, Dirac, Fisher, and Klein-Gordon [6–8]. Since many PDE types lack exact solutions, a variety of analytical and numerical techniques are described to introduce approximate solutions for both linear and nonlinear PDEs [9, 10]. These techniques include the Laplace transforms (LT) approach [11], Fourier transform technique [12], homotopy perturbation and analysis method [13–15], operational calculus method [16], operational matrix method [17], Adomian decomposition method [18], the residual power series (RPS) method [19], and variational iteration method [20]. Fractional-order differential equations have emerged as powerful tools for modeling complex dynamical systems in diverse fields such as fluid mechanics, wave propagation, and control theory. Recent advancements have focused on developing analytical and numerical methods to explore the behavior of these systems. Studies like Alshammari et al. [21] and Qin et al. [22] have highlighted innovative approaches for solving fractional-order nonlinear systems, while others, such as Alderremy et al. [23], have employed series solutions to tackle reaction-diffusion models. The exploration of coupled systems, as presented by Al-Sawalha et al. [24], and soliton solutions for perturbed equations, as investigated by Yasmin et al. [25], demonstrates the breadth of applications for fractional calculus. Furthermore, techniques for controlling fractional evolution equations [26] and analyzing fractional Navier-Stokes equations [27] have significantly advanced the field. Recent works continue to extend these methodologies to electrical engineering [28–30], nonlinear control systems [31, 32], and predictive modeling [34, 35]. These contributions underscore the growing importance and versatility of fractional-order systems in solving real-world problems across various disciplines.

The advection-dispersion equation (ADE) is derived from the study of particle dispersion and advection occurring simultaneously when particles move in a fluid according to Brownian motion. Since solute transport in anomalous diffusion is faster than the estimated square root of time provided by Baeumer et al. [36], the fractional ADE (FADE) provides a better description of the phenomena of anomalous diffusion of particles in the transport process. Numerous environmental problems have been studied using this equation, including groundwater contamination, chemical solute diffusion, smoke and dust pollution of the atmosphere, and pollutant discharges [37]. Thus, a number of academics are

becoming interested in FADE.

$$D_{\Omega}^{p}\Psi(\Phi,\Omega) - k\,a\frac{\partial^2\Psi(\Phi,\Omega)}{\partial\Phi^2} + j\frac{\partial\Psi(\Phi,\Omega)}{\partial\Phi} = 0, \text{ where } 0 < p \leq 1. \tag{1.1}$$

where Ω is time, Φ is the spatial domain, Ψ is the solute concentration, k, j are the average dispersion coefficient and fluid velocity, and "a" is the parameter that determines the order of the time-fractional derivatives and the space-fractional derivatives. We look at the fractional derivative in the Caputo sense. The generic response expression has parameters that govern the order of fractional derivatives, and these parameters can be varied to produce a variety of outcomes. When p = 1, the fractional equation reduces to the typical ADE. The basic solutions of the ADE over time will be Gaussian densities whose variances and means depend on the values of the macroscopic transport coefficients k and j. The space-time FADE has already been examined by several writers.

The residual power series method (RPSM) was founded by Omar Abu Arqub [38] in 2013. It is created by combining the Taylor series with the residual error function. An infinite convergence series provides a solution to DEs. The study of fractional-order differential equations continues to gain prominence due to their ability to model systems with memory and hereditary properties. Innovative analytical and numerical methods have been developed to address these equations, such as the iterative techniques presented by Arqub et al. [39] and El-Ajou et al. [40]. Residual power series methods have proven effective for constructing solutions, as demonstrated by Xu et al. [41] and Zhang et al. [42]. Additionally, the analysis of physical models with temporal and spatial memory effects [43, 44], as well as bifurcation studies of fractional systems [45], highlights the versatility of fractional calculus in capturing complex dynamics. Recent advancements, including hybrid techniques like Laplace transform combined with power series approaches [46–48], further extend the applicability of these methods to nonlinear and multidimensional systems. These contributions underline the significant progress in solving fractional problems across various fields, from physics to engineering.

In this work, we introduce a novel approach that combines the RPSM with the Mohand transform to approximate solutions to FADEs. It is evident that this computational series provides an accurate solution after only a limited number of iterations, and the resulting series converges rapidly.

A key challenge with existing methodologies is the computational complexity and the substantial effort required for their implementation. Our contribution is the development of a new iterative approach for solving FADEs, termed the Mohand transform iterative method (MTIM). By incorporating the Mohand transform into this iterative process, we reduce both the computational complexity and the required effort, offering a more efficient solution.

In this paper, we solve the FADEs using both the Mohand RPSM (MRPSM) and MTIM. Through comparison with other numerical techniques, we demonstrate that these methods outperform existing approaches in terms of accuracy. A detailed comparison analysis of the numerical results further supports the effectiveness and reliability of the proposed methods. The appeal of fractional-order derivatives increases as their value rises, and our algorithms are fast, accurate, user-friendly, and resilient to computational errors. This advancement will aid mathematicians in solving a wide range of PDEs more effectively.

2. Mohand transform key concepts

An overview of the Mohand transform (MT) and its key concepts will be given below to lay the groundwork for this process.

Definition 2.1. The MT is defined by the integral equation:

$$M\{\Psi(\Omega)\} = s^2 \int_0^{\infty} e^{-s\Omega}\Psi(\Omega)d\Omega = \Phi(s)$$

Definition 2.2. The inverse MT is given by:

$$\Psi(\Omega) = M^{-1}\{\Phi(s)\} = \frac{1}{2\pi i}\int_{c-i\infty}^{c+i\infty} \frac{1}{s^2}e^{s\Omega}\Phi(s)ds, \quad c \in R$$

where M^{-1} is the inverse operator of MT.

Definition 2.3. [50]: The MT equation has the following fractional derivative:

$$M[\Psi^p(\Omega)] = s^p R(s) - \sum_{k=0}^{n-1} \frac{\Psi^k(0)}{s^{k-(p+1)}},\ 0 < p \leq n$$

Definition 2.4. Some of the features relating to MT are as follows:

1. $M[\Psi'(\Omega)] = sR(s) - s^2R(0)$,
2. $M[\Psi''(\Omega)] = s^2R(s) - s^3R(0) - s^2R'(0)$,
3. $M[\Psi^n(\Omega)] = s^nR(s) - s^{n+1}R(0) - s^nR'(0) - \cdots - s^nR^{n-1}(0)$.

Lemma 2.1. $\Psi(\Phi, \Omega)$ *denotes the exponential order function. The equation* $M[R(s)] = \Psi(\Phi, \Omega)$ *describes the MT in this context.*

$$M[D_{\Omega}^{rp}\Psi(\Phi, \Omega)] = s^{rp}R(s) - \sum_{j=0}^{r-1} s^{p(r-j)-1}D_{\Omega}^{jp}\Psi(\Phi, 0), 0 < p \leq 1, \tag{2.1}$$

where $\Phi = (\Phi_1, \Phi_2, \cdots, \Phi_p) \in \mathbb{R}^p$, $p \in \mathbb{N}$, and $D_{\Omega}^{rp} = D_{\Omega}^{p}.D_{\Omega}^{p}.\cdots.D_{\Omega}^{p}(r - times)$

Proof. Using mathematical induction, it is feasible to verify Eq 2.1. The subsequent results are obtained when $r = 1$ is placed into Eq 2.1:

$$M[D_{\Omega}^{2p}\Psi(\Phi, \Omega)] = s^{2p}R(s) - s^{2p-1}\Psi(\Phi, 0) - s^{p-1}D_{\Omega}^{p}\Psi(\Phi, 0).$$

The definition 2.3 indicates that Eq 2.1 is valid for $r = 1$. When $r = 2$ is substituted into Eq 2.1, we get:

$$M[D_{r}^{2p}\Psi(\Phi, \Omega)] = s^{2p}R(s) - s^{2p-1}\Psi(\Phi, 0) - s^{p-1}D_{\Omega}^{p}\Psi(\Phi, 0). \tag{2.2}$$

Using Eq 2.2 left-hand side (L.H.S), the resulting expression is achieved.

$$L.H.S = M[D_{\Omega}^{2p}\Psi(\Phi, \Omega)]. \tag{2.3}$$

Equation 2.3 can also be written as:

$$L.H.S = M[D_{\Omega}^{p}\Psi(\Phi,\Omega)]. \tag{2.4}$$

Assume

$$z(\Phi,\Omega) = D_{\Omega}^{p}\Psi(\Phi,\Omega). \tag{2.5}$$

Hence, Eq 2.4 becomes

$$L.H.S = M[D_{\Omega}^{p}z(\Phi,\Omega)]. \tag{2.6}$$

The Caputo derivative leads to the modification of Eq 2.6.

$$L.H.S = M[J^{1-p}z^{'}(\Phi,\Omega)]. \tag{2.7}$$

The Riemann-Liouville (R-L) integral for MT is given by Eq 2.7, from which more details can be derived:

$$L.H.S = \frac{M[z^{'}(\Phi,\Omega)]}{s^{1-p}}. \tag{2.8}$$

By employing the differentiability characteristic of the MT, the subsequent expression of Eq 2.8 is derived:

$$L.H.S = s^{p}Z(\Phi,s) - \frac{z(\Phi,0)}{s^{1-p}}, \tag{2.9}$$

Equation 2.5 is employed to obtain the following outcome.

$$Z(\Phi,s) = s^{p}R(s) - \frac{\Psi(\Phi,0)}{s^{1-p}},$$

In this case, $M[z(\Omega,\Phi)] = Z(\Phi,s)$. Thus, Eq 2.9 is modified to the following form:

$$L.H.S = s^{2p}R(s) - \frac{\Psi(\Phi,0)}{s^{1-2p}} - \frac{D_{\Omega}^{p}\Psi(\Phi,0)}{s^{1-p}}, \tag{2.10}$$

For $r = K$, both Eqs 2.1 and 2.10 are consistent. Suppose that for $r = K$, Eq 2.1 is true. So, put $r = K$ in Eq 2.1

$$M[D_{\Omega}^{Kp}\Psi(\Phi,\Omega)] = s^{Kp}R(s) - \sum_{j=0}^{K-1} s^{p(K-j)-1}D_{\Omega}^{jp}D_{\Omega}^{jp}\Psi(\Phi,0),\ 0 < p \leq 1. \tag{2.11}$$

Finally, we have to show that Eq 2.1 is true for $r = K + 1$. We may write Eq 2.1 as:

$$M[D_{\Omega}^{(K+1)p}\Psi(\Phi,\Omega)] = s^{(K+1)p}R(s) - \sum_{j=0}^{K} s^{p((K+1)-j)-1}D_{\Omega}^{jp}\Psi(\Phi,0). \tag{2.12}$$

The following outcome is obtained by examining the left side of Eq 2.12.

$$L.H.S = M[D_{\Omega}^{Kp}(D_{\Omega}^{Kp})]. \tag{2.13}$$

Let

$$D_{\Omega}^{Kp} = g(\Phi,\Omega).$$

From Eq 2.13, we obtain:

$$L.H.S = M[D_{\Omega}^{p} g(\Phi, \Omega)]. \tag{2.14}$$

Eq 2.14 can yield the subsequent outcome by employing the R-L integral and the Caputo derivative.

$$L.H.S = s^{p} M[D_{\Omega}^{Kp} \Psi(\Phi, \Omega)] - \frac{g(\Phi, 0)}{s^{1-p}}. \tag{2.15}$$

By utilizing Eq 2.11, it is feasible to get Eq 2.15.

$$L.H.S = s^{rp} R(s) - \sum_{j=0}^{r-1} s^{p(r-j)-1} D_{\Omega}^{jp} \Psi(\Phi, 0), \tag{2.16}$$

This result was obtained by solving the Eq 2.16.

$$L.H.S = M[D_{\Omega}^{rp} \Psi(\Phi, 0)].$$

It is proved that Eq 2.1 is true for $r = K + 1$. Therefore, Eq 2.1 is valid for all positive integers when the mathematical induction method is applied. □

Lemma 2.2. *Let the function $\Psi(\Phi, \Omega)$ be exponential order and the MT be $\Psi(\Phi, \Omega)$ is $M[\Psi(\Phi, \Omega)] = R(s)$. Then, the following is the MT representation in the multiple fractional Taylor series (MFTS) form:*

$$R(s) = \sum_{r=0}^{\infty} \frac{\hbar_r(\Phi)}{s^{rp+1}}, s > 0, \tag{2.17}$$

where, $\Phi = (s_1, \Phi_2, \cdots, \Phi_p) \in \mathbb{R}^p,\ p \in \mathbb{N}$.

Proof. Suppose this form of Taylor's series:

$$\Psi(\Phi, \Omega) = \hbar_0(\Phi) + \hbar_1(\Phi) \frac{\Omega^p}{\Gamma[p+1]} + +\hbar_2(\Phi) \frac{\Omega^{2p}}{\Gamma[2p+1]} + \cdots. \tag{2.18}$$

We obtain the following outcome when MT is applied on Eq 2.18:

$$M\left[\Psi(\Phi, \Omega)\right] = M\left[\hbar_0(\Phi)\right] + M\left[\hbar_1(\Phi) \frac{\Omega^p}{\Gamma[p+1]}\right] + M\left[\hbar_1(\Phi) \frac{\Omega^{2p}}{\Gamma[2p+1]}\right] + \cdots$$

When the MT's features are utilized, the following results are obtained:

$$M\left[\Psi(\Phi, \Omega)\right] = \hbar_0(\Phi) \frac{1}{s} + \hbar_1(\Phi) \frac{\Gamma[p+1]}{\Gamma[p+1]} \frac{1}{s^{p+1}} + \hbar_2(\Phi) \frac{\Gamma[2p+1]}{\Gamma[2p+1]} \frac{1}{s^{2p+1}} \cdots$$

As a result, an MT-specific form of Taylor's series is produced, denoted as Eq 2.17. □

Lemma 2.3. *$M[\Psi(\Phi, \Omega)] = R(s)$ is the new form of Taylor's series 2.17, which is used to represent the multiple fractional power series (MFPS).*

$$\hbar_0(\Phi) = \lim_{s \to \infty} sR(s) = \Psi(\Phi, 0). \tag{2.19}$$

Proof. The modified new form of Taylor's series is as follows:

$$\hbar_0(\Phi) = sR(s) - \frac{\hbar_1(\Phi)}{s^p} - \frac{\hbar_2(\Phi)}{s^{2p}} - \cdots \tag{2.20}$$

The required solution, which can be determined as $lim_{x\to\infty}$, is implemented through Eq 2.19 and a short computation, as illustrated in 2.20. □

Theorem 2.4. *Consider the function $M[\Psi(\Phi, \Omega)]$, then the $R(s)$ denoted in MFPS form is given below:*

$$R(s) = \sum_{r=0}^{\infty} \frac{\hbar_r(\Phi)}{s^{rp+1}}, \ s > 0,$$

where $\Phi = (\Phi_1, \Phi_2, \cdots, \Phi_p) \in \mathbb{R}^p$ and $p \in \mathbb{N}$. Then, we have

$$\hbar_r(\Phi) = D_r^{rp}\Psi(\Phi, 0),$$

where, $D_\Omega^{rp} = D_\Omega^p.D_\Omega^p.\cdots.D_\Omega^p(r - times)$.

Proof. Consider the Taylor series:

$$\hbar_1(\Phi) = s^{p+1}R(s) - s^p\hbar_0(\Phi) - \frac{\hbar_2(\Phi)}{s^p} - \frac{\hbar_3(\Phi)}{s^{2p}} - \cdots \tag{2.21}$$

Taking $\lim_{s\to\infty}$ of Eq 2.21 to deduce:

$$\hbar_1(\Phi) = \lim_{s\to\infty}(s^{p+1}R(s) - s^p\hbar_0(\Phi)) - \lim_{s\to\infty}\frac{\hbar_2(\Phi)}{s^p} - \lim_{s\to\infty}\frac{\hbar_3(\Phi)}{s^{2p}} - \cdots$$

we get the following equality by taking the limit:

$$\hbar_1(\Phi) = \lim_{s\to\infty}(s^{p+1}R(s) - s^p\hbar_0(\Phi)). \tag{2.22}$$

Lemma 2.1 and Eq 2.22 are used to get the following outcome:

$$\hbar_1(\Phi) = \lim_{s\to\infty}(sM[D_\Omega^p\Psi(\Phi, \Omega)](s)). \tag{2.23}$$

Eq 2.23 is further modified using Lemma 2.2:

$$\hbar_1(\Phi) = D_\Omega^p\Psi(\Phi, 0).$$

By employing the $\lim_{s\to\infty}$ and using Taylor series once more, we deduce:

$$\hbar_2(\Phi) = s^{2p+1}R(s) - s^{2p}\hbar_0(\Phi) - s^p\hbar_1(\Phi) - \frac{\hbar_3(\Phi)}{s^p} - \cdots$$

Lemma 2.2 is used to obtain:

$$\hbar_2(\Phi) = \lim_{s\to\infty} s(s^{2p}R(s) - s^{2p-1}\hbar_0(\Phi) - s^{p-1}\hbar_1(\Phi)). \tag{2.24}$$

In a specific way, we use Eq 2.3 and Lemma 2.1 to make the following changes in Eq 2.24:

$$\hbar_2(\Phi) = D_{\Omega}^{2p}\Psi(\Phi, 0).$$

Using the same process, we can get:

$$\hbar_3(\Phi) = \lim_{s\to\infty} s(M[D_{\Omega}^{2p}\Psi(\Phi, p)](s)).$$

To obtain the final result, we use Lemma 2.3:

$$\hbar_3(\Phi) = D_{\Omega}^{3p}\Psi(\Phi, 0).$$

Generally,

$$\hbar_r(\Phi) = D_{\Omega}^{rp}\Psi(\Phi, 0).$$

Proved. □

The following theorem contains a description and illustration of the concepts that affect the convergence of the modified version of Taylor's series.

Theorem 2.5. *In Lemma 2.2, a formula for MFTS is provided and can be expressed as follows:* $M[\Psi(\Omega, \Phi)] = R(s)$. *When* $|s^a M[D_{\Omega}^{(K+1)p}\Psi(\Phi, \Omega)]| \leq T$, *for all* $s > 0$ *and* $0 < p \leq 1$, *the residual* $H_K(\Phi, s)$ *of the new MFTS satisfied the inequality:*

$$|H_K(\Phi, s)| \leq \frac{T}{s^{(K+1)p+1}}, \ s > 0.$$

Proof. Consider $M[D_{\Omega}^{rp}\Psi(\Phi, \Omega)](s)$ is defined on $s > 0$ for $r = 0, 1, 2, \cdots, K+1$ and suppose $|sM[D_{\Omega^{K+1}}\Psi(\Phi, \Omega)]| \leq T$. This relationship can be found by employing the revised Taylor's series:

$$H_K(\Phi, s) = R(s) - \sum_{r=0}^{K} \frac{\hbar_r(\Phi)}{s^{rp+1}}. \tag{2.25}$$

Theorem 2.4 is employed to transform Eq 2.25.

$$H_K(\Phi, s) = R(s) - \sum_{r=0}^{K} \frac{D_{\Omega}^{rp}\Psi(\Phi, 0)}{s^{rp+1}}. \tag{2.26}$$

To resolve this problem, multiply both sides by $s^{(K+1)a+1}$ in order to obtain:

$$s^{(K+1)p+1}H_K(\Phi, s) = s(s^{(K+1)p}R(s) - \sum_{r=0}^{K} s^{(K+1-r)p-1}D_{\Omega}^{rp}\Psi(\Phi, 0)). \tag{2.27}$$

Lemma 2.1 is applied to Eq 2.27 to obtain the subsequent result:

$$s^{(K+1)p+1}H_K(\Phi, s) = sM[D_{\Omega}^{(K+1)p}\Psi(\Phi, \Omega)]. \tag{2.28}$$

Calculating the absolute value of Eq 2.28 yields the following:

$$|s^{(K+1)p+1}H_K(\Phi, s)| = |sM[D_{\Omega}^{(K+1)p}\Psi(\Phi, \Omega)]|. \tag{2.29}$$

The subsequent result is obtained by using the condition from Eq 2.29.

$$\frac{-T}{s^{(K+1)p+1}} \leq H_K(\Phi, s) \leq \frac{T}{s^{(K+1)p+1}}. \tag{2.30}$$

From Eq 2.30, we get.

$$|H_K(\Phi, s)| \leq \frac{T}{s^{(K+1)p+1}}.$$

In this way, a novel condition for the series' convergence is established. □

3. Road map of MT combination with RPSM method

This section outlines the process of constructing the MT with RPSM in order to provide an approximate solution to PDEs.

Step 1: Consider the PDE:

$$D_{\Omega}^{p}\Psi(\Phi, \Omega) + \vartheta(\Phi)N(\Psi) - \delta(\Phi, \Psi) = 0, \tag{3.1}$$

Step 2: Taking the MT of Eq 3.1 to obtain:

$$M[D_{\Omega}^{p}\Psi(\Phi, \Omega) + \vartheta(\Phi)N(\Psi) - \delta(\Phi, \Psi)] = 0, \tag{3.2}$$

Using Lemma 2.1, we can get the following result:

$$R(s) = \sum_{j=0}^{q-1} \frac{D_{\Omega}^{j}\Psi(\Phi, 0)}{s^{jp+1}} - \frac{\vartheta(\Phi)Y(s)}{s^{jp}} + \frac{F(\Phi, s)}{s^{jp}}, \tag{3.3}$$

where, $M[\delta(\Phi, \Psi)] = F(\Phi, s), M[N(\Psi)] = Y(s)$.

Step 3: Solving Eq 3.3, we deduce:

$$R(s) = \sum_{r=0}^{\infty} \frac{\hbar_r(\Phi)}{s^{rp+1}}, \ s > 0,$$

Step 4: Now, use the following procedure to obtain the solution:

$$\hbar_0(\Phi) = \lim_{s\to\infty} sR(s) = \Psi(\Phi, 0),$$

Utilize Theorem 2.5 to get the subsequent result:

$$\hbar_1(\Phi) = D_{\Omega}^{p}\Psi(\Phi, 0),$$

$$\hbar_2(\Phi) = D_{\Omega}^{2p}\Psi(\Phi, 0),$$

$$\vdots$$

$$\hbar_w(\Phi) = D_{\Omega}^{wp}\Psi(\Phi, 0),$$

Step 5: To get the K^{th} truncated series $R(s)$, apply the following formula:

$$R_K(s) = \sum_{r=0}^{K} \frac{\hbar_r(\Phi)}{s^{rp+1}},\ s > 0,$$

$$R_K(s) = \frac{\hbar_0(\Phi)}{s} + \frac{\hbar_1(\Phi)}{s^{p+1}} + \cdots + \frac{\hbar_w(\Phi)}{s^{wp+1}} + \sum_{r=w+1}^{K} \frac{\hbar_r(\Phi)}{s^{rp+1}},$$

Step 6: Determine the following by calculating the Mohand residual function (MRF) from 3.3 separately of the K^{th}-truncated Mohand residual function:

$$MRes(\Phi, s) = R(s) - \sum_{j=0}^{q-1} \frac{D_\Omega^j \Psi(\Phi, 0)}{s^{jp+1}} + \frac{\vartheta(\Phi)Y(s)}{s^{jp}} - \frac{F(\Phi, s)}{s^{jp}},$$

and

$$MRes_K(\Phi, s) = R_K(s) - \sum_{j=0}^{q-1} \frac{D_\Omega^j \Psi(\Phi, 0)}{s^{jp+1}} + \frac{\vartheta(\Phi)Y(s)}{s^{jp}} - \frac{F(\Phi, s)}{s^{jp}}. \tag{3.4}$$

Step 7: Instead of its expansion form, Eq 3.4 can be formulated in terms of $R_K(s)$.

$$\begin{aligned} MRes_K(\Phi, s) &= \Big(\frac{\hbar_0(\Phi)}{s} + \frac{\hbar_1(\Phi)}{s^{p+1}} + \cdots + \frac{\hbar_w(\Phi)}{s^{wp+1}} + \sum_{r=w+1}^{K} \frac{\hbar_r(\Phi)}{s^{rp+1}}\Big) \\ &- \sum_{j=0}^{q-1} \frac{D_\Omega^j \Psi(\Phi, 0)}{s^{jp+1}} + \frac{\vartheta(\Phi)Y(s)}{s^{jp}} - \frac{F(\Phi, s)}{s^{jp}}. \end{aligned} \tag{3.5}$$

Step 8: Multiplying s^{Kp+1} with Eq 3.5:

$$\begin{aligned} s^{Kp+1} MRes_K(\Phi, s) &= s^{Kp+1}\Big(\frac{\hbar_0(\Phi)}{s} + \frac{\hbar_1(\Phi)}{s^{p+1}} + \cdots + \frac{\hbar_w(\Phi)}{s^{wp+1}} + \sum_{r=w+1}^{K} \frac{\hbar_r(\Phi)}{s^{rp+1}} \\ &- \sum_{j=0}^{q-1} \frac{D_\Omega^j \Psi(\Phi, 0)}{s^{jp+1}} + \frac{\vartheta(\Phi)Y(s)}{s^{jp}} - \frac{F(\Phi, s)}{s^{jp}}\Big). \end{aligned} \tag{3.6}$$

Step 9: Taking $\lim_{s\to\infty}$ of Eq 3.6 to obtain:

$$\begin{aligned} \lim_{s\to\infty} s^{Kp+1} MRes_K(\Phi, s) &= \lim_{s\to\infty} s^{Kp+1}\Big(\frac{\hbar_0(\Phi)}{s} + \frac{\hbar_1(\Phi)}{s^{p+1}} + \cdots + \frac{\hbar_w(\Phi)}{s^{wp+1}} + \sum_{r=w+1}^{K} \frac{\hbar_r(\Phi)}{s^{rp+1}} \\ &- \sum_{j=0}^{q-1} \frac{D_\Omega^j \Psi(\Phi, 0)}{s^{jp+1}} + \frac{\vartheta(\Phi)Y(s)}{s^{jp}} - \frac{F(\Phi, s)}{s^{jp}}\Big). \end{aligned}$$

Step 10: $\hbar_K(\Phi)$ values can be obtained using Eq 3.6.

$$\lim_{s\to\infty}(s^{Kp+1} MRes_K(\Phi, s)) = 0,$$

where $K = 1 + w, 2 + w, \cdots$.

Step 11: The K^{th}-approximation of Eq 3.3 is obtained by substituting $\hbar_K(\Phi)$ with a K-truncated series of $R(s)$.

Step 12: The final solution $\Psi_K(\Phi, \Omega)$ is obtained using the inverse operator of MT.

3.1. New iterative method combined with MT

Consider the following PDE:

$$D_{\Omega}^{p}\Psi(\Phi,\Omega) = \Upsilon\Big(\Psi(\Phi,\Omega), D_{\Phi}^{\Omega}\Psi(\Phi,\Omega), D_{\Phi}^{2\Omega}\Psi(\Phi,\Omega), D_{\Phi}^{3\Omega}\Psi(\Phi,\Omega)\Big),\ 0 < p,\Omega \leq 1, \tag{3.7}$$

Initial conditions

$$\Psi^{(k)}(\Phi,0) = h_k,\ k = 0,1,2,\cdots,m-1, \tag{3.8}$$

with $\Psi(\Phi,\Omega)$ denoting the function that we are required to identify, while $\Upsilon\Big(\Psi(\Phi,\Omega), D_{\Phi}^{\Omega}\Psi(\Phi,\Omega)$ $, D_{\Phi}^{2\Omega}\Psi(\Phi,\Omega), D_{\Phi}^{3\Omega}\Psi(\Phi,\Omega)\Big)$ are nonlinear or linear operators of $\Psi(\Phi,\Omega), D_{\Phi}^{\Omega}\Psi(\Phi,\Omega), D_{\Phi}^{2\Omega}\Psi(\Phi,\Omega)$ and $D_{\Phi}^{3\Omega}\Psi(\Phi,\Omega)$. The expression that follows is obtained by applying the MT to both sides of Equation 3.7.

$$M[\Psi(\Phi,\Omega)] = \frac{1}{s^p}\Big(\sum_{k=0}^{m-1}\frac{\Psi^{(k)}(\Phi,0)}{s^{1-p+k}} + M\Big[\Upsilon\Big(\Psi(\Phi,\Omega), D_{\Phi}^{\Omega}\Psi(\Phi,\Omega), D_{\Phi}^{2\Omega}\Psi(\Phi,\Omega), D_{\Phi}^{3\Omega}\Psi(\Phi,\Omega)\Big)\Big]\Big), \tag{3.9}$$

The inverse MT gives the subsequent result in this case:

$$\Psi(\Phi,\Omega) = M^{-1}\Big[\frac{1}{s^p}\Big(\sum_{k=0}^{m-1}\frac{\Psi^{(k)}(\Phi,0)}{s^{1-p+k}} + M\Big[\Upsilon\Big(\Psi(\Phi,\Omega), D_{\Phi}^{\Omega}\Psi(\Phi,\Omega), D_{\Phi}^{2\Omega}\Psi(\Phi,\Omega), D_{\Phi}^{3\Omega}\Psi(\Phi,\Omega)\Big)\Big]\Big)\Big]. \tag{3.10}$$

The MTIM gives the infinite series solution as given below.

$$\Psi(\Phi,\Omega) = \sum_{i=0}^{\infty}\Psi_i. \tag{3.11}$$

The operators $\Upsilon\Big(\Psi, D_{\Phi}^{\Omega}\Psi, D_{\Phi}^{2\Omega}\Psi, D_{\Phi}^{3\Omega}\Psi\Big)$ decompose as given below:

$$\begin{aligned}\Upsilon\Big(\Psi, D_{\Phi}^{\Omega}\Psi, D_{\Phi}^{2\Omega}\Psi, D_{\Phi}^{3\Omega}\Psi\Big) &= \Upsilon\Big(\Psi_0, D_{\Phi}^{\Omega}\Psi_0, D_{\Phi}^{2\Omega}\Psi_0, D_{\Phi}^{3\Omega}\Psi_0\Big)\\ &+ \sum_{i=0}^{\infty}\left(\Upsilon\Big(\sum_{k=0}^{i}\Big(\Psi_k, D_{\Phi}^{\Omega}\Psi_k, D_{\Phi}^{2\Omega}\Psi_k, D_{\Phi}^{3\Omega}\Psi_k\Big)\Big) - \Upsilon\Big(\sum_{k=1}^{i-1}\Big(\Psi_k, D_{\Phi}^{\Omega}\Psi_k, D_{\Phi}^{2\Omega}\Psi_k, D_{\Phi}^{3\Omega}\Psi_k\Big)\Big)\right).\end{aligned} \tag{3.12}$$

By substituting the values of Eq 3.11 and Eq 3.12 in Eq 3.10, the subsequent equation can be obtained.

$$\begin{aligned}\sum_{i=0}^{\infty}\Psi_i(\Phi,\Omega) &= M^{-1}\Big[\frac{1}{s^p}\Big(\sum_{k=0}^{m-1}\frac{\Psi^{(k)}(\Phi,0)}{s^{2-p+k}} + M[\Upsilon(\Psi_0, D_{\Phi}^{\Omega}\Psi_0, D_{\Phi}^{2\Omega}\Psi_0, D_{\Phi}^{3\Omega}\Psi_0)]\Big)\Big]\\ &+ M^{-1}\Big[\frac{1}{s^p}\Big(M\Big[\sum_{i=0}^{\infty}\Big(\Upsilon\sum_{k=0}^{i}(\Psi_k, D_{\Phi}^{\Omega}\Psi_k, D_{\Phi}^{2\Omega}\Psi_k, D_{\Phi}^{3\Omega}\Psi_k)\Big)\Big]\Big)\Big]\\ &- M^{-1}\Big[\frac{1}{s^p}\Big(M\Big[\Big(\Upsilon\sum_{k=1}^{i-1}(\Psi_k, D_{\Phi}^{\Omega}\Psi_k, D_{\Phi}^{2\Omega}\Psi_k, D_{\Phi}^{3\Omega}\Psi_k)\Big)\Big]\Big)\Big]\end{aligned} \tag{3.13}$$

$$\begin{aligned}
&\Psi_0(\Phi,\Omega) = M^{-1}\Big[\frac{1}{s^p}\Big(\sum_{k=0}^{m-1}\frac{\Psi^{(k)}(\Phi,0)}{s^{2-p+k}}\Big)\Big],\\
&\Psi_1(\Phi,\Omega) = M^{-1}\Big[\frac{1}{s^p}\Big(M[\Upsilon(\Psi_0, D_\Phi^\Omega\Psi_0, D_\Phi^{2\Omega}\Psi_0, D_\Phi^{3\Omega}\Psi_0)]\Big)\Big],\\
&\vdots\\
&\Psi_{i+1}(\Phi,\Omega) = M^{-1}\Big[\frac{1}{s^p}\Big(M\Big[\sum_{i=0}^{\infty}\Big(\Upsilon\sum_{k=0}^{i}(\Psi_k, D_\Phi^\Omega\Psi_k, D_\Phi^{2\Omega}\Psi_k, D_\Phi^{3\Omega}\Psi_k)\Big)\Big]\Big)\Big]\\
&- M^{-1}\Big[\frac{1}{s^p}\Big(M\Big[\Big(\Upsilon\sum_{k=1}^{i-1}(\Psi_k, D_\Phi^\Omega\Psi_k, D_\Phi^{2\Omega}\Psi_k, D_\Phi^{3\Omega}\Psi_k)\Big)\Big]\Big)\Big],\ i = 1,2,\cdots.
\end{aligned} \tag{3.14}$$

The following expression can be used to obtain the i-terms of Eq 3.7 analytically:

$$\Psi(\Phi,\Omega) = \sum_{i=0}^{m-1}\Psi_i. \tag{3.15}$$

4. Applications

4.1. Problem 1 solution using MRPSM

Suppose the following time FADE:

$$D_\Omega^p\Psi(\Phi,\Omega) - a\frac{\partial^2\Psi(\Phi,\Omega)}{\partial\Phi^2} + \frac{\partial\Psi(\Phi,\Omega)}{\partial\Phi} = 0,\ \text{where}\ \ 0 < p \le 1. \tag{4.1}$$

Initial condition

$$\Psi(\Phi,0) = e^{-\Phi}, \tag{4.2}$$

and exact solution

$$\Psi(\Phi,\Omega) = e^{(a+1)\Omega-\Phi}. \tag{4.3}$$

Eq 4.2 and the MT are used to get the following result from Eq 4.1.

$$\Psi(\Phi,s) - \frac{e^{-\Phi}}{s} - \frac{a}{s^p}\Big[\frac{\partial^2\Psi(\Phi,s)}{\partial\Phi^2}\Big] + \frac{1}{s^p}\Big[\frac{\partial\Psi(\Phi,s)}{\partial\Phi}\Big] = 0. \tag{4.4}$$

The k^{th} terms of the series that are truncated are:

$$\Psi(\Phi,s) = \frac{e^{-\Phi}}{s} + \sum_{r=1}^{k}\frac{f_r(\Phi,s)}{s^{rp+1}},\ \ r = 1,2,3,4\cdots. \tag{4.5}$$

Residual Mohand function is given by:

$$\mathcal{M}_\Omega Res(\Phi,s) = \Psi(\Phi,s) - \frac{e^{-\Phi}}{s} - \frac{a}{s^p}\Big[\frac{\partial^2\Psi(\Phi,s)}{\partial\Phi^2}\Big] + \frac{1}{s^p}\Big[\frac{\partial\Psi(\Phi,s)}{\partial\Phi}\Big] = 0, \tag{4.6}$$

and the k^{th}-MRFs as:

$$\mathcal{M}_{\Omega}Res_k(\Phi, s) = \Psi_k(\Phi, s) - \frac{e^{-\Phi}}{s} - \frac{a}{s^p}\Big[\frac{\partial^2\Psi_k(\Phi, s)}{\partial\Phi^2}\Big] + \frac{1}{s^p}\Big[\frac{\partial\Psi_k(\Phi, s)}{\partial\Phi}\Big] = 0. \tag{4.7}$$

The following procedures should be implemented to determine the value of $f_r(\Phi, s)$ for $r = 1, 2, 3, ...$: replace the r^{th}-Mohand residual function Eq 4.7 for the r^{th}-truncated series Eq 4.5, and multiply the expression by s^{rp+1} for solving the relation, $\lim_{s\to\infty}(s^{rp+1})M_{\Omega}Res_{\Psi,r}(\Phi, s)) = 0$ for $r = 1, 2, 3, \cdots$. Some terms that we obtain are as follows:

$$f_1(\Phi, s) = (a + 1)e^{-\Phi}, \tag{4.8}$$

$$f_2(\Phi, s) = (a + 1)^2e^{-\Phi}, \tag{4.9}$$

$$f_3(\Phi, s) = (a + 1)^3e^{-\Phi}, \tag{4.10}$$

$$f_4(\Phi, s) = (a + 1)^4e^{-\Phi}, \tag{4.11}$$

and so on.
To obtain the desired result, the function $f_r(\Phi, s)$ should be substituted into Eq (4.5).

$$\Psi(\Phi, s) = \frac{e^{-\Phi}}{s} + \frac{(a + 1)e^{-\Phi}}{s^{p+1}} + \frac{(a + 1)^2e^{-\Phi}}{s^{2p+1}} + \frac{(a + 1)^3e^{-\Phi}}{s^{3p+1}} + \frac{(a + 1)^4e^{-\Phi}}{s^{4p+1}} + \cdots. \tag{4.12}$$

Apply the inverse operator of MT to obtain the final solution:

$$\Psi(\Phi, \Omega) = e^{-\Phi} + \frac{(a + 1)\Omega^p e^{-\Phi}}{\Gamma(p + 1)} + \frac{(a + 1)^2\Omega^{2p} e^{-\Phi}}{\Gamma(2p + 1)} + \frac{(a + 1)^3\Omega^{3p} e^{-\Phi}}{\Gamma(3p + 1)} + \frac{(a + 1)^4\Omega^{4p} e^{-\Phi}}{\Gamma(4p + 1)} + \cdots. \tag{4.13}$$

4.2. Problem 1 solution using MTIM

Suppose the following time FADE:

$$D^p_{\Omega}\Psi(\Phi, \Omega) = a\frac{\partial^2\Psi(\Phi, \Omega)}{\partial\Phi^2} - \frac{\partial\Psi(\Phi, \Omega)}{\partial\Phi}, \text{ where } 0 < p \leq 1. \tag{4.14}$$

Initial condition

$$\Psi(\Phi, 0) = e^{-\Phi}. \tag{4.15}$$

Apply the MT on Eq 4.14:

$$M[D^p_{\Omega}\Psi(\Phi, \Omega)] = \frac{1}{s^p}\Big(\sum_{k=0}^{m-1}\frac{\Psi^{(k)}(\Phi, 0)}{s^{2-p+k}} + M\Big[a\frac{\partial^2\Psi(\Phi, \Omega)}{\partial\Phi^2} - \frac{\partial\Psi(\Phi, \Omega)}{\partial\Phi}\Big)\Big]\Big). \tag{4.16}$$

Apply the inverse operator of MT on Eq 4.16:

$$\Psi(\Phi, \Omega) = M^{-1}\Big[\frac{1}{s^p}\Big(\sum_{k=0}^{m-1}\frac{\Psi^{(k)}(\Phi, \eta, 0)}{s^{2-p+k}} + M\Big[a\frac{\partial^2\Psi(\Phi, \Omega)}{\partial\Phi^2} - \frac{\partial\Psi(\Phi, \Omega)}{\partial\Phi}\Big]\Big)\Big]. \tag{4.17}$$

Iteratively utilize the MT to get the following result:

$$\begin{aligned}\Psi_0(\Phi,\Omega) &= M^{-1}\Big[\frac{1}{s^p}\Big(\sum_{k=0}^{m-1}\frac{\Psi^{(k)}(\Phi,0)}{s^{2-p+k}}\Big)\Big]\\ &= M^{-1}\Big[\frac{\Psi(\Phi,0)}{s^2}\Big]\\ &= e^{-\Phi}.\end{aligned}$$

Eq 4.14 is solved using the R-L integral to obtain:

$$\Psi(\Phi,\Omega) = e^{-\Phi} + M\Big[a\frac{\partial^2\Psi(\Phi,\Omega)}{\partial\Phi^2} - \frac{\partial\Psi(\Phi,\Omega)}{\partial\Phi}\Big]. \tag{4.18}$$

Some of the terms that the MITM method produce are as follows:

$$\Psi_0(\Phi,\Omega) = e^{-\Phi}, \tag{4.19}$$

$$\Psi_1(\Phi,\Omega) = \frac{(a+1)\Omega^p e^{-\Phi}}{\Gamma(p+1)}, \tag{4.20}$$

$$\Psi_2(\Phi,\Omega) = \frac{(a+1)^2\Omega^{2p} e^{-\Phi}}{\Gamma(2p+1)}, \tag{4.21}$$

$$\Psi_3(\Phi,\Omega) = \frac{(a+1)^3\Omega^{3p} e^{-\Phi}}{\Gamma(3p+1)}, \tag{4.22}$$

$$\Psi_4(\Phi,\Omega) = \frac{(a+1)^4\Omega^{4p} e^{-\Phi}}{\Gamma(4p+1)}. \tag{4.23}$$

The final solution is:

$$\Psi(\Phi,\Omega) = \Psi_0(\Phi,\Omega) + \Psi_1(\Phi,\Omega) + \Psi_2(\Phi,\Omega) + \Psi_3(\Phi,\Omega) + \Psi_4(\Phi,\Omega) + \cdots, \tag{4.24}$$

$$\Psi(\Phi,\Omega) = e^{-\Phi} + \frac{(a+1)\Omega^p e^{-\Phi}}{\Gamma(p+1)} + \frac{(a+1)^2\Omega^{2p} e^{-\Phi}}{\Gamma(2p+1)} + \frac{(a+1)^3\Omega^{3p} e^{-\Phi}}{\Gamma(3p+1)} + \frac{(a+1)^4\Omega^{4p} e^{-\Phi}}{\Gamma(4p+1)} + \cdots. \tag{4.25}$$

Table 1 presents the error comparison between the solutions obtained using the MRPSM and the MTIM for the function $\Psi(\Phi,\Omega)$. This comparison highlights the accuracy of both methods, where the error values demonstrate that the MTIM and MRPSM provide very close approximations to the exact solution, with MTIM showing slightly lower error in most cases. Figure 1 displays the exact and approximate solutions of $\Psi(\Phi,\Omega)$, for $p = 1$ and $\Omega = 0.1$. Panel (a) presents the exact solution, providing a clear benchmark for comparison, while panel (b) shows the approximate solution obtained using the proposed methods. The graphical comparison indicates that the approximation closely matches the exact solution, highlighting the effectiveness of the methods in capturing the underlying dynamics of the system. Figure 2 offers a side-by-side comparison of the exact and approximate solutions of $\Psi(\Phi,\Omega)$, for $p = 1$ and $\Omega = 0.1$. Panel (a) shows the exact solution, while panel (b) illustrates the approximate solution. The slight deviations between the two solutions in the graph are due to the inherent approximation process, but the overall agreement between them emphasizes the

reliability and accuracy of both MRPSM and MTIM. Figure 3 presents a 3D graphical representation of the approximate solution for p of $\Psi(\Phi, \Omega)$, for $\Omega = 0.1$. The 3D plot effectively illustrates how the solution varies with respect to both, providing a visual understanding of the solution's behavior for varying fractional orders. The surface plot reveals smooth transitions and complex interactions between the variables, demonstrating the robustness of the methods in handling fractional-order differential equations. Figure 4 shows a 2D graphical representation of the approximate solution for different values of p of $\Psi(\Phi, \Omega)$, for $\Omega = 0.1$ is presented for multiple fractional orders. The 2D plots highlight how the solution's shape changes with different values of p, providing further insight into the dynamics of fractional systems. The consistency in the graphs demonstrates the stability of the methods over varying parameters. Overall, the graphical results confirm the accuracy and reliability of the MRPSM and MTIM in approximating solutions to the FADEs, providing a comprehensive visual understanding of the solution behavior across different conditions.

Table 1. MRPSM and MTIM solution absolute error with exact solution for $\Psi(\Phi, \Omega)$ of problem 1.

		$MRPSM$	$MRPSM$	$MRPSM$	$MRPSM$	$MRPSM$	$MTIM$
Ω	Φ	$Error_{p=0.1}$	$Error_{p=0.2}$	$Error_{p=0.3}$	$Error_{p=0.4}$	$Error_{p=0.5}$	$Error_{p=0.5}$
0.01	0	1.8771808	0.8154997	0.4094808	0.2235174	0.1262354	0.1262354
	1	0.6905762	0.3000055	0.1506395	0.0822274	0.0464394	0.0464394
	2	0.2540487	0.1103658	0.0554172	0.0302497	0.0170841	0.0170841
	3	0.0934593	0.0406013	0.0203868	0.0111282	0.0062848	0.0062848
	4	0.0343817	0.0149363	0.0074999	0.0040938	0.0023120	0.0023120
	5	0.0126483	0.0054947	0.0027590	0.0015060	0.0008505	0.0008505
0.05	0	2.6258573	1.4029278	0.7966979	0.4774295	0.2945283	0.2945283
	1	0.9659989	0.5161082	0.2930888	0.1756365	0.1083509	0.1083509
	2	0.3553711	0.1898656	0.1078213	0.0646130	0.0398600	0.0398600
	3	0.1307337	0.0698476	0.0396652	0.0237698	0.0146637	0.0146637
	4	0.0480942	0.0256955	0.0145920	0.0087444	0.0053944	0.0053944
	5	0.0176928	0.0094528	0.0053681	0.0032168	0.0019845	0.0019845
0.10	0	3.0338831	1.8058633	1.0962378	0.6851275	0.4362119	0.4362119
	1	1.1161032	0.6643399	0.4032833	0.2520443	0.1604734	0.1604734
	2	0.4105914	0.2443970	0.1483596	0.0927219	0.0590348	0.0590348
	3	0.1510481	0.0899086	0.0545784	0.0341104	0.0217177	0.0217177
	4	0.0555675	0.0330755	0.0200782	0.0125485	0.0079895	0.0079895
	5	0.0204421	0.0121678	0.0073863	0.0046163	0.0029391	0.0029391

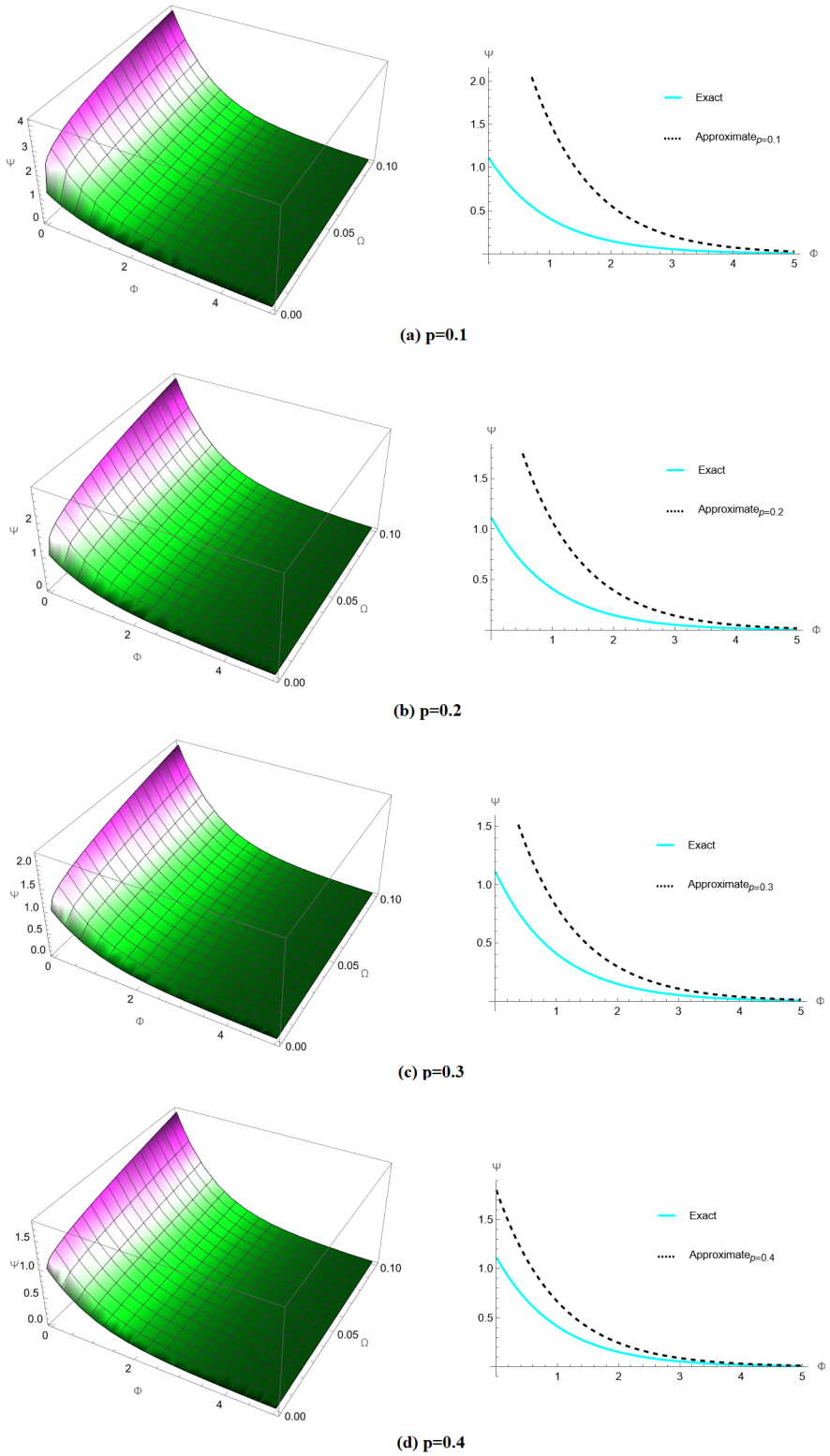

Figure 1. Graphical representation of approximate solution and exact solution for different values of p of $\Psi(\Phi, \Omega)$ for $\Omega = 0.1$.

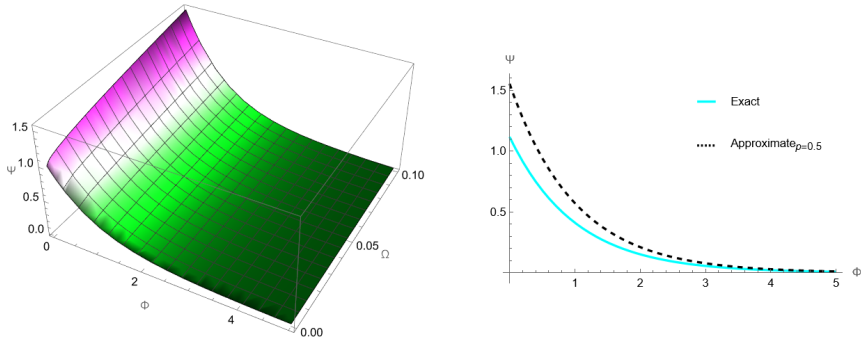

(e) p=0.5

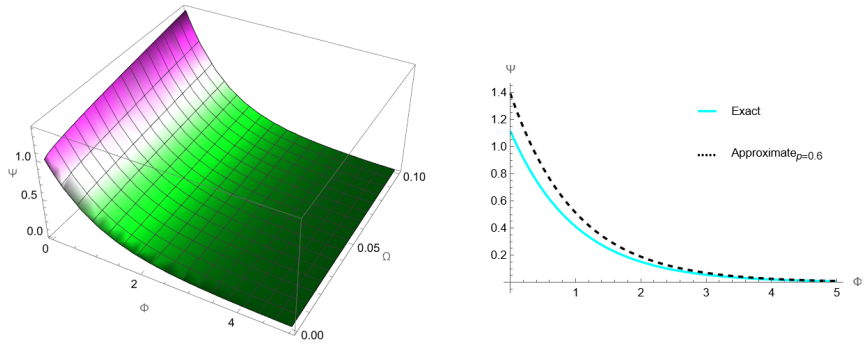

(f) p=0.6

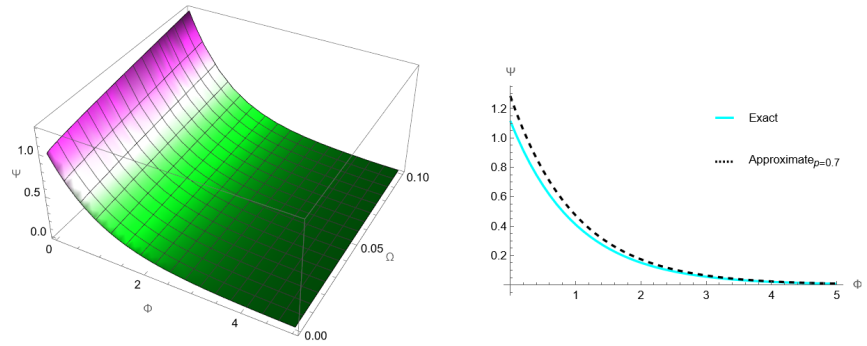

(g) p=0.7

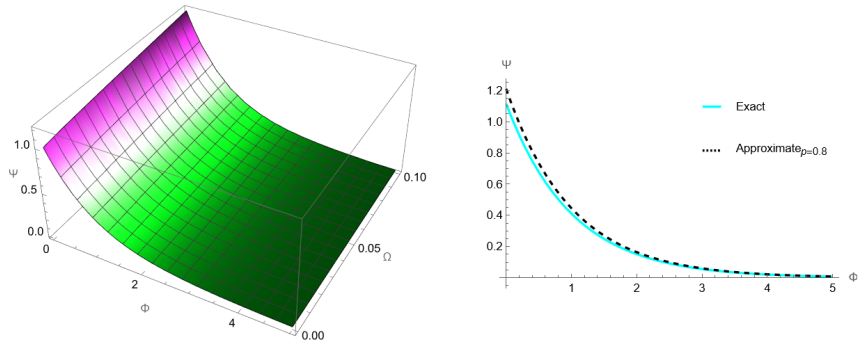

(h) p=0.8

Figure 2. Graphical representation of approximate solution and exact solution for different values of p of $\Psi(\Phi, \Omega)$ for $\Omega = 0.1$.

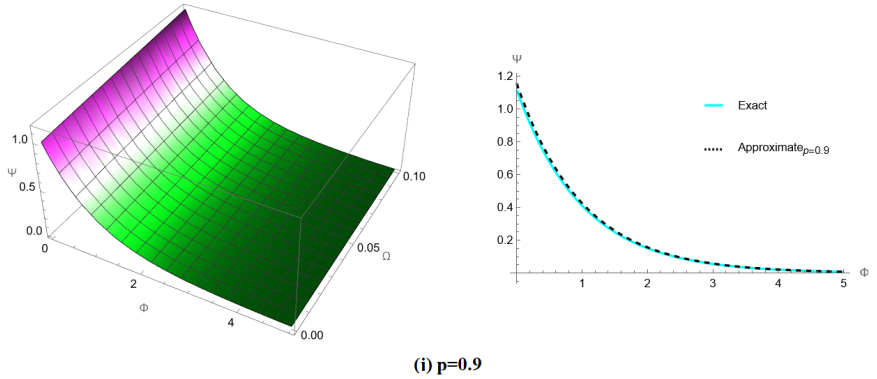

(i) p=0.9

Figure 3. Graphical representation of approximate solution and exact solution for $p = 0.9$ of $\Psi(\Phi, \Omega)$ for $\Omega = 0.1$.

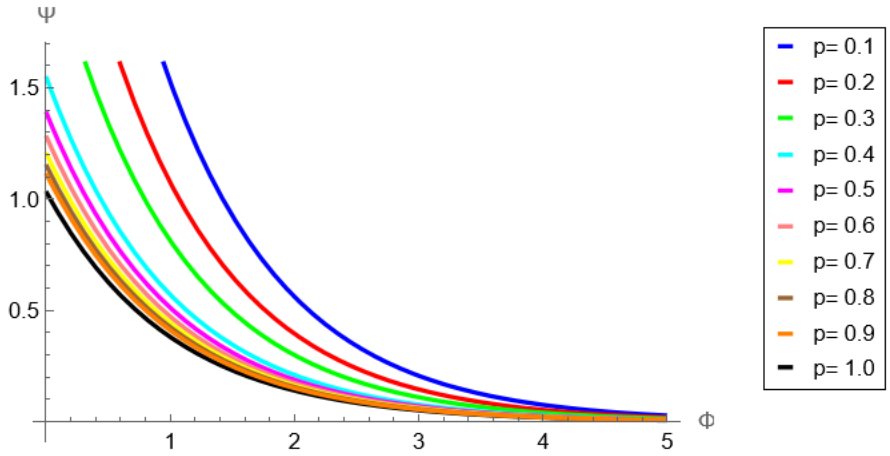

Figure 4. 2D comparison of approximate solution for different values of p of $\Psi(\Phi, \Omega)$ for $\Omega = 0.1$.

Table 2 provides a solution comparison for the fractional order p of $\Psi(\Phi, \Omega)$ using both the MRPSM and the MTIM for $\Omega = 0.1$. The comparison reveals that both methods yield highly similar results, with slight variations depending on the fractional order p. This table reinforces the reliability and accuracy of both methods in approximating the solution, showing that both MRPSM and MTIM are effective in solving fractional-order differential equations. Figure 5 illustrates the solutions of $\Psi(\Phi, \Omega)$ for $p = 1$ and $\Omega = 0.1$ using both MRPSM and MTIM. Panel (a) shows the MRPSM solution, while panel (b) presents the MTIM solution. Both graphs exhibit nearly identical solution profiles, demonstrating the consistency between the two methods. The solutions are smooth and exhibit the expected characteristics of the FADEs, confirming that both methods provide accurate approximations. Figure 6 provides a side-by-side comparison of the MRPSM and MTIM solutions for $\Psi(\Phi, \Omega)$ for $p = 1$ and $\Omega = 0.1$. Panel (a) shows the MRPSM solution, while panel (b) shows the MTIM solution. The visual comparison reinforces the earlier finding that both methods produce nearly identical results, validating that MTIM and MRPSM are robust and reliable for this problem. The solutions' close

agreement further suggests that either method can be used for efficient computation of FADEs.

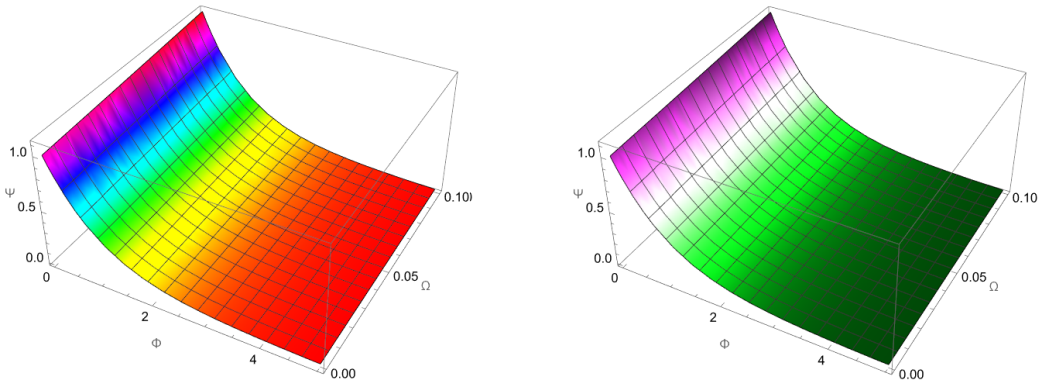

Figure 5. (a) Exact solution and (b) approximate solution of $\Psi(\Phi, \Omega)$ for $p = 1$ and $\Omega = 0.1$.

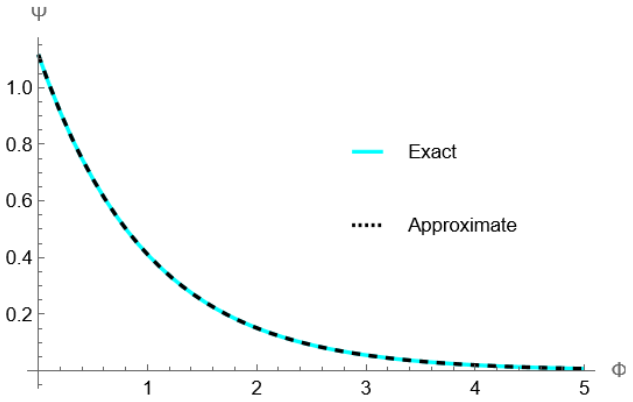

Figure 6. (a) Exact solution and (b) approximate solution comparison of $\Psi(\Phi, \Omega)$ for $p = 1$ and $\Omega = 0.1$.

Table 2. MRPSM and MTIM solution absolute error with exact solution for $\Psi(\Phi, \Omega)$ of problem 1.

		MRPSM	*MRPSM*	*MRPSM*	*MRPSM*	*MRPSM*	*MTIM*
Ω	Φ	$Error_{p=0.6}$	$Error_{p=0.7}$	$Error_{p=0.8}$	$Error_{p=0.9}$	$Error_{p=1.0}$	$Error_{p=1.0}$
0.01	0	0.0711952	0.0387171	0.0191468	0.0072487	1.344480×10^{-12}	1.344480×10^{-12}
	1	0.0261912	0.0142432	0.0070437	0.0026666	4.946598×10^{-13}	4.946598×10^{-13}
	2	0.0096352	0.0052397	0.0025912	0.0009810	1.819377×10^{-13}	1.819377×10^{-13}
	3	0.0035446	0.0019276	0.0009532	0.0003608	6.694644×10^{-14}	6.694644×10^{-14}
	4	0.0013039	0.0007091	0.0003506	0.0001327	2.463307×10^{-14}	2.463307×10^{-14}
	5	0.0004797	0.0002608	0.0001290	0.0000488	9.061328×10^{-15}	9.061328×10^{-15}
0.05	0	0.1816240	0.1080370	0.0583301	0.0240053	4.232785×10^{-9}	4.232785×10^{-9}
	1	0.0668158	0.0397445	0.0214584	0.0088310	1.557154×10^{-9}	1.557154×10^{-9}
	2	0.0245802	0.0146212	0.0078941	0.0032487	5.728452×10^{-10}	5.728452×10^{-10}
	3	0.0090425	0.0053788	0.0029040	0.0011951	2.107380×10^{-10}	2.107380×10^{-10}
	4	0.0033265	0.0019787	0.0010683	0.0004396	7.752618×10^{-11}	7.752618×10^{-11}
	5	0.0012237	0.0007279	0.0003930	0.0001617	2.852028×10^{-11}	2.852028×10^{-11}
0.10	0	0.2767880	0.1693540	0.0940604	0.0398121	1.367088×10^{-7}	1.3670887×10^{-7}
	1	0.1018250	0.0623018	0.0346029	0.0146460	5.029238×10^{-8}	5.0292383×10^{-8}
	2	0.0374592	0.0229195	0.0127297	0.0053879	1.850153×10^{-8}	1.8501533×10^{-8}
	3	0.0137805	0.0084316	0.0046829	0.0019821	6.806333×10^{-9}	6.8063339×10^{-9}
	4	0.0050695	0.0031018	0.0017227	0.0007291	2.503910×10^{-9}	2.5039103×10^{-9}
	5	0.0018649	0.0011411	0.0006337	0.0002682	9.211371×10^{-10}	9.2113713×10^{-10}

4.3. Problem 2 solution using MRPSM

Suppose the following time FADE:

$$D^{p}_{\Omega}\Psi(\Phi,\Omega) - a\frac{\partial^2\Psi(\Phi,\Omega)}{\partial\Phi^2} + \frac{\partial\Psi(\Phi,\Omega)}{\partial\Phi} = 0, \text{ where } 0 < p \leq 1. \tag{4.26}$$

Initial condition

$$\Psi(\Phi, 0) = \Phi^3 - \Phi^2, \tag{4.27}$$

Eq 4.27 and the MT is used to get the following result from Eq (4.26).

$$\Psi(\Phi, s) - \frac{\Phi^3 - \Phi^2}{s} - \frac{a}{s^p}\Big[\frac{\partial^2\Psi(\Phi, s)}{\partial\Phi^2}\Big] + \frac{1}{s^p}\Big[\frac{\partial\Psi(\Phi, s)}{\partial\Phi}\Big] = 0. \tag{4.28}$$

The k^{th} terms of the series that are truncated are:

$$\Psi(\Phi, s) = \frac{\Phi^3 - \Phi^2}{s} + \sum_{r=1}^{k}\frac{f_r(\Phi, s)}{s^{rp+1}}, \quad r = 1, 2, 3, 4\cdots. \tag{4.29}$$

Residual Mohand function is given by:

$$\mathcal{M}_{\Omega}Res(\Phi, s) = \Psi(\Phi, s) - \frac{\Phi^3 - \Phi^2}{s} - \frac{a}{s^p}\Big[\frac{\partial^2\Psi(\Phi, s)}{\partial\Phi^2}\Big] + \frac{1}{s^p}\Big[\frac{\partial\Psi(\Phi, s)}{\partial\Phi}\Big] = 0, \tag{4.30}$$

and the k^{th}-MRFs as:

$$\mathcal{M}_{\Omega}Res_k(\Phi, s) = \Psi_k(\Phi, s) - \frac{\Phi^3 - \Phi^2}{s} - \frac{a}{s^p}\Big[\frac{\partial^2\Psi_k(\Phi, s)}{\partial\Phi^2}\Big] + \frac{1}{s^p}\Big[\frac{\partial\Psi_k(\Phi, s)}{\partial\Phi}\Big] = 0. \tag{4.31}$$

The following procedures should be implemented to determine the value of $f_r(\Phi, s)$ for $r = 1, 2, 3, ...$: replace the r^{th}-Mohand residual function Eq 4.31 for the r^{th}-truncated series Eq 4.29, and multiply the expression by s^{rp+1} for solving the relation, $\lim_{s\to\infty}(s^{rp+1})M_{\Omega}Res_{\Psi,r}(\Phi, s)) = 0$ for $r = 1, 2, 3, \cdots$. Some terms that we obtain are as follows:

$$f_1(\Phi, s) = a(6\Phi - 2) + \Phi(2 - 3\Phi), \tag{4.32}$$

$$f_2(\Phi, s) = -12a + 6\Phi - 2, \tag{4.33}$$

$$f_3(\Phi, s) = -6, \tag{4.34}$$

$$f_4(\Phi, s) = 0, \tag{4.35}$$

and so on.
To obtain the desired result, the function $f_r(\Phi, s)$ should be substituted into Eq (4.29).

$$\Psi(\Phi, s) = \frac{\Phi^3 - \Phi^2}{s} + \frac{a(6\Phi - 2) + \Phi(2 - 3\Phi)}{s^{p+1}} + \frac{-12a + 6\Phi - 2}{s^{2p+1}} - \frac{6}{s^{3p+1}} + \frac{0}{s^{4p+1}} + \cdots. \tag{4.36}$$

Apply the inverse operator of MT to obtain the final solution:

$$\Psi(\Phi, \Omega) = (\Phi - 1)\Phi^2 + \frac{(a(6\Phi - 2) + \Phi(2 - 3\Phi))\Omega^p}{\Gamma(p + 1)} - \frac{2(6a - 3\Phi + 1)\Omega^{2p}}{\Gamma(2p + 1)} - \frac{6\Omega^{3p}}{\Gamma(3p + 1)} + \cdots. \tag{4.37}$$

4.4. Problem 2 solution using MTIM

Suppose the following time FADE:

$$D^p_{\Omega}\Psi(\Phi, \Omega) = a\frac{\partial^2\Psi(\Phi, \Omega)}{\partial\Phi^2} - \frac{\partial\Psi(\Phi, \Omega)}{\partial\Phi}, \text{ where } 0 < p \leq 1. \tag{4.38}$$

Initial condition

$$\Psi(\Phi, 0) = \Phi^3 - \Phi^2. \tag{4.39}$$

Apply the MT on Eq 4.38:

$$M[D^p_{\Omega}\Psi(\Phi, \Omega)] = \frac{1}{s^p}\Big(\sum_{k=0}^{m-1}\frac{\Psi^{(k)}(\Phi, 0)}{s^{2-p+k}} + M\Big[a\frac{\partial^2\Psi(\Phi, \Omega)}{\partial\Phi^2} - \frac{\partial\Psi(\Phi, \Omega)}{\partial\Phi}\Big)\Big]\Big). \tag{4.40}$$

Apply the inverse operator of MT on Eq 4.40:

$$\Psi(\Phi, \Omega) = M^{-1}\Big[\frac{1}{s^p}\Big(\sum_{k=0}^{m-1}\frac{\Psi^{(k)}(\Phi, \eta, 0)}{s^{2-p+k}} + M\Big[a\frac{\partial^2\Psi(\Phi, \Omega)}{\partial\Phi^2} - \frac{\partial\Psi(\Phi, \Omega)}{\partial\Phi}\Big]\Big)\Big]. \tag{4.41}$$

Iteratively utilize the MT to get the following result:

$$\begin{aligned}\Psi_0(\Phi,\Omega) &= M^{-1}\Big[\frac{1}{s^p}\Big(\sum_{k=0}^{m-1}\frac{\Psi^{(k)}(\Phi,0)}{s^{2-p+k}}\Big)\Big]\\ &= M^{-1}\Big[\frac{\Psi(\Phi,0)}{s^2}\Big]\\ &= \Phi^3-\Phi^2.\end{aligned}$$

Eq 4.38 is solved using the R-L integral to obtain:

$$\Psi(\Phi,\Omega) = \Phi^3-\Phi^2+M\Big[a\frac{\partial^2\Psi(\Phi,\Omega)}{\partial\Phi^2}-\frac{\partial\Psi(\Phi,\Omega)}{\partial\Phi}\Big]. \tag{4.42}$$

Some of the terms that the MITM method produces are as follows:

$$\Psi_0(\Phi,\Omega) = \Phi^3-\Phi^2, \tag{4.43}$$

$$\Psi_1(\Phi,\Omega) = \frac{(a(6\Phi-2)+\Phi(2-3\Phi))\Omega^p}{\Gamma(p+1)}, \tag{4.44}$$

$$\Psi_2(\Phi,\Omega) = -\frac{2(6a-3\Phi+1)\Omega^{2p}}{\Gamma(2p+1)}, \tag{4.45}$$

$$\Psi_3(\Phi,\Omega) = -\frac{6\Omega^{3p}}{\Gamma(3p+1)}, \tag{4.46}$$

$$\Psi_4(\Phi,\Omega) = 0. \tag{4.47}$$

The final solution is:

$$\Psi(\Phi,\Omega) = \Psi_0(\Phi,\Omega)+\Psi_1(\Phi,\Omega)+\Psi_2(\Phi,\Omega)+\Psi_3(\Phi,\Omega)+\Psi_4(\Phi,\Omega)+\cdots, \tag{4.48}$$

$$\Psi(\Phi,\Omega) = (\Phi-1)\Phi^2+\frac{(a(6\Phi-2)+\Phi(2-3\Phi))\Omega^p}{\Gamma(p+1)}-\frac{2(6a-3\Phi+1)\Omega^{2p}}{\Gamma(2p+1)}-\frac{6\Omega^{3p}}{\Gamma(3p+1)}+\cdots. \tag{4.49}$$

Figure 7 presents a 3D graphical representation of the approximate solution for $\Psi(\Phi,\Omega)$ for $p = 1$ and $\Omega = 0.1$ constant. The 3D plot effectively demonstrates how the solution changes as the fractional order p varies. The surface reveals the intricate relationships between p and the solution, showcasing how the solution becomes more complex with increasing fractional order. This 3D representation highlights the flexibility of the methods in handling different fractional orders.

Figure 8 shows a 2D graphical representation of the approximate solution for varying fractional orders p of $\Psi(\Phi,\Omega)$ for $\Omega = 0.1$. The 2D plots provide a clearer view of the solutions dependence on the fractional order p, allowing for an intuitive understanding of how the solution evolves as p changes. These plots help visualize the impact of fractional derivatives on the solution and demonstrate the power of both MRPSM and MTIM in modeling fractional systems. Figure 9, graphical representation of approximate solution for different values of p of $\Psi(\Phi,\Omega)$ for $\Omega = 0.1$. Figure 10, (a) MRPSM solution and (b) MTIM solution of $\Psi(\Phi,\Omega)$ for $p = 1$ and $\Omega = 0.1$. Figure 11, (a) MRPSM solution

and (b) MTIM solution comparison of $\Psi(\Phi, \Omega)$ for $p = 1$ and $\Omega = 0.1$. Table 3, the approximate solution comparison for the fractional order p of $\Psi(\Phi, \Omega)$ for $\Omega = 0.1$ of problem 2. Table 4, the approximate solution comparison for the fractional order p of $\Psi(\Phi, \Omega)$ for $\Omega = 0.1$ of problem 2.

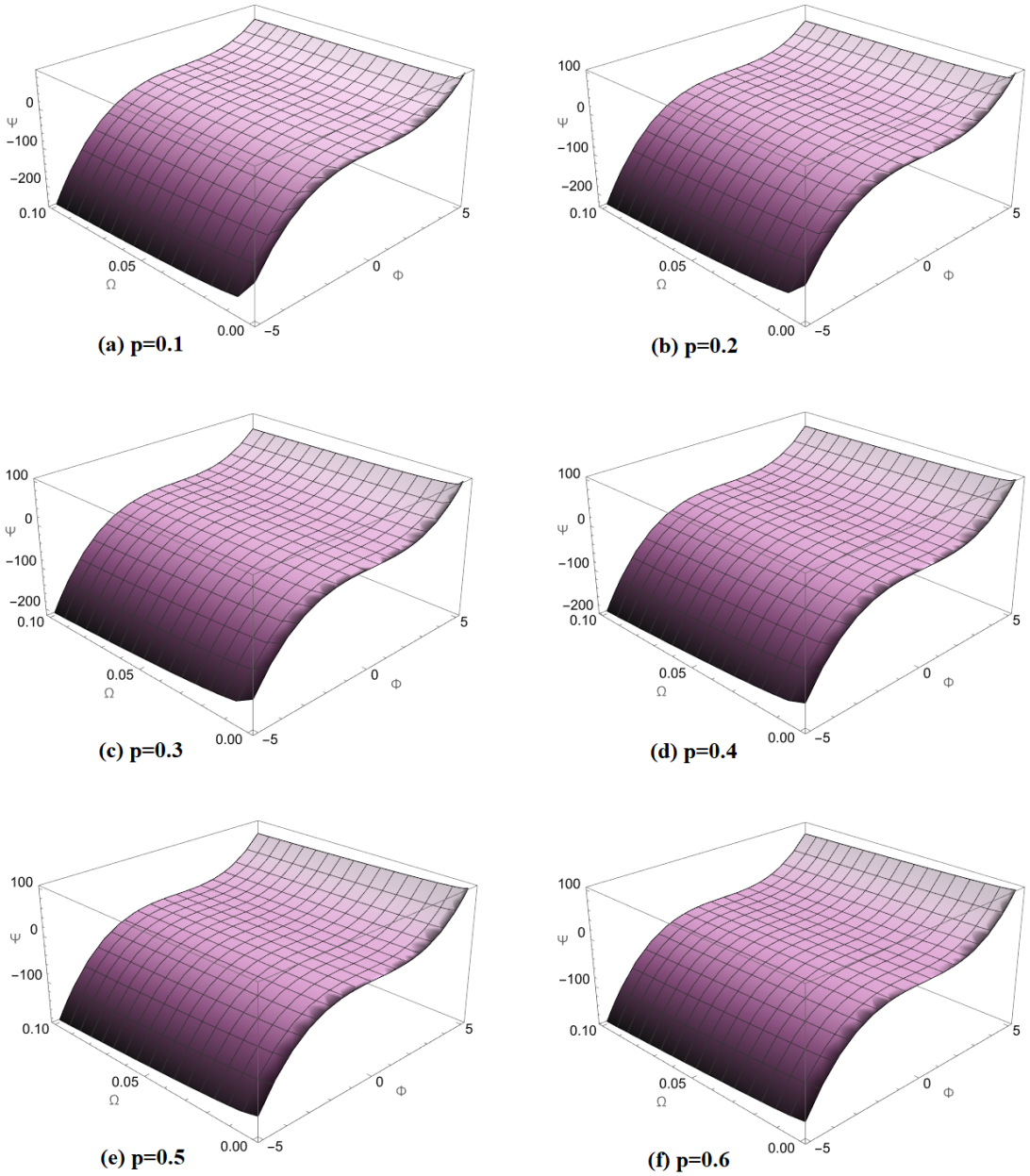

Figure 7. Graphical representation of approximate solution for different values of p of $\Psi(\Phi, \Omega)$ for $\Omega = 0.1$.

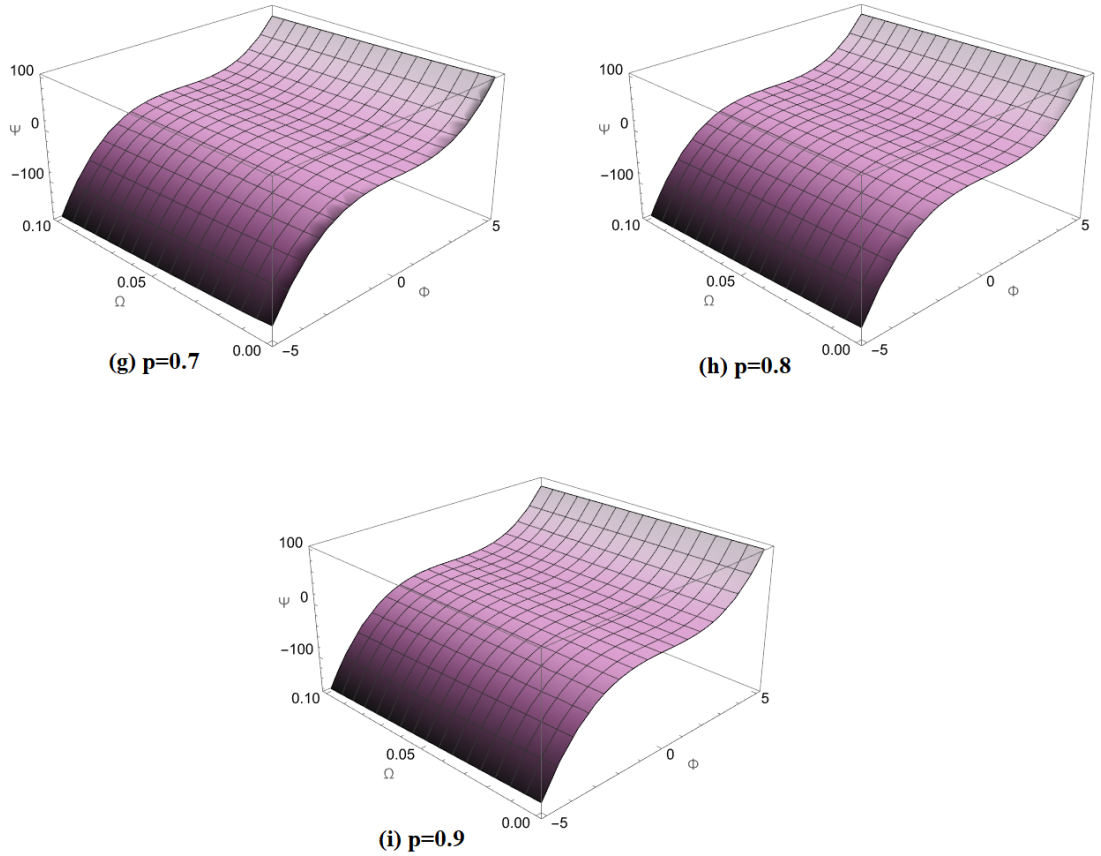

Figure 8. Graphical representation of approximate solution for different values of p of $\Psi(\Phi, \Omega)$ for $\Omega = 0.1$.

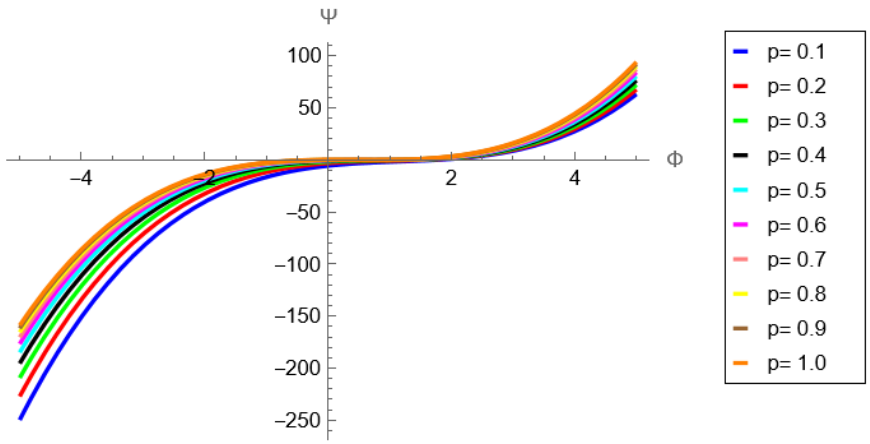

Figure 9. Graphical representation of approximate solution for different values of p of $\Psi(\Phi, \Omega)$ for $\Omega = 0.1$.

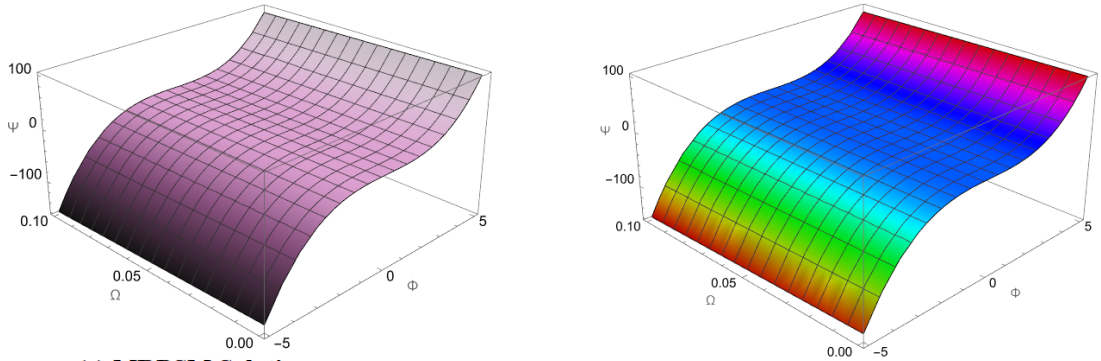

Figure 10. (a) MRPSM solution and (b) MTIM solution of $\Psi(\Phi, \Omega)$ for $p = 1$ and $\Omega = 0.1$.

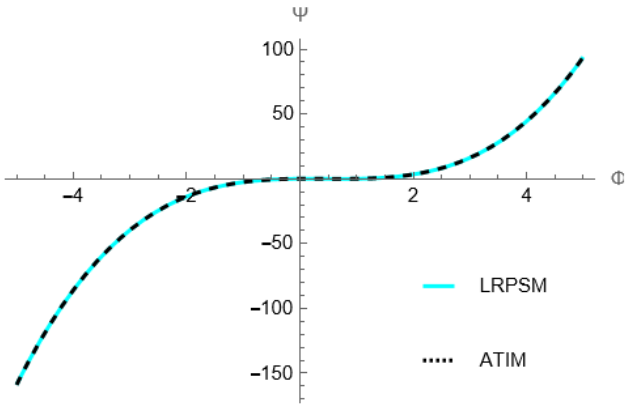

Figure 11. (a) MRPSM solution and (b) MTIM solution comparison of $\Psi(\Phi, \Omega)$ for $p = 1$ and $\Omega = 0.1$.

Table 3. The approximate solution comparison for the fractional order p of $\Psi(\Phi, \Omega)$ for $\Omega = 0.1$ of problem 2.

Φ	$MRPSM_{p=0.1}$	$MRPSM_{p=0.2}$	$MRPSM_{p=0.3}$	$MRPSM_{p=0.4}$	$MRPSM_{p=0.5}$	$MTIM_{p=0.5}$
0.1	-4.2739432	-2.2705525	-1.1345749	-0.5412512	-0.2480652	-0.2480652
0.2	-3.7877746	-1.9446238	-0.9241210	-0.4101038	-0.1696735	-0.1696735
0.3	-3.3597029	-1.6679266	-0.7551737	-0.3138778	-0.1206913	-0.1206913
0.4	-2.9837281	-1.4344608	-0.6217331	-0.2465733	-0.0951186	-0.0951186
0.5	-2.6538501	-1.2382265	-0.5177991	-0.2021903	-0.0869554	-0.0869554
0.6	-2.3640690	-1.0732237	-0.4373717	-0.1747287	-0.0902017	-0.0902017
0.7	-2.1083848	-0.9334523	-0.3744510	-0.1581885	-0.0988575	-0.0988575
0.8	-1.8807974	-0.8129124	-0.3230370	-0.1465699	-0.1069227	-0.1069227
0.9	-1.6753069	-0.7056040	-0.2771295	-0.1338726	-0.1083975	-0.1083975
1.0	-1.4859133	-0.6055270	-0.2307288	-0.1140968	-0.0972817	-0.0972817

Table 4. The approximate solution comparison for the fractional order p of $\Psi(\Phi, \Omega)$ for $\Omega = 0.1$ of problem 2.

Φ	$MRPSM_{p=0.6}$	$MRPSM_{p=0.7}$	$MRPSM_{p=0.8}$	$MRPSM_{p=0.9}$	$MRPSM_{p=1.0}$	$MTIM_{p=1.0}$
0.1	-0.1089106	-0.0451462	-0.0171733	-0.0058199	-0.0020000	-0.0020000
0.2	-0.0649407	-0.0234443	-0.0098919	-0.0079637	-0.0104000	-0.0104000
0.3	-0.0458382	-0.0229178	-0.0208205	-0.0259612	-0.0328000	-0.0328000
0.4	-0.0456031	-0.0375666	-0.0439590	-0.0538126	-0.0632000	-0.0632000
0.5	-0.0582355	-0.0613906	-0.0733075	-0.0855179	-0.0956000	-0.0956000
0.6	-0.0777353	-0.0883899	-0.1028658	-0.1150770	-0.1239999	-0.1239999
0.7	-0.0981026	-0.1125645	-0.1266341	-0.1364899	-0.1424000	-0.1424000
0.8	-0.1133373	-0.1279144	-0.1386123	-0.1437566	-0.1448000	-0.1448000
0.9	-0.1174395	-0.1284395	-0.1328005	-0.1308772	-0.1252000	-0.1252000
1.0	-0.1044091	-0.1081400	-0.1031985	-0.0918517	-0.0776000	-0.0776000

4.5. Problem 3 solution using MRPSM

Suppose the following time FADE:

$$D^p_{\Omega}\Psi(\Phi, \Omega) - a\frac{\partial^2\Psi(\Phi, \Omega)}{\partial\Phi^2} + \frac{\partial\Psi(\Phi, \Omega)}{\partial\Phi} = 0, \text{ where } 0 < p \leq 1. \tag{4.50}$$

Initial condition

$$\Psi(\Phi, 0) = \cos(\Phi), \tag{4.51}$$

Eq 4.51 and the MT are used to get the following result from Eq 4.50.

$$\Psi(\Phi, s) - \frac{\cos(\Phi)}{s} - \frac{a}{s^p}\Big[\frac{\partial^2\Psi(\Phi, s)}{\partial\Phi^2}\Big] + \frac{1}{s^p}\Big[\frac{\partial\Psi(\Phi, s)}{\partial\Phi}\Big] = 0. \tag{4.52}$$

The k^{th} terms of the series that are truncated are:

$$\Psi(\Phi, s) = \frac{\cos(\Phi)}{s} + \sum_{r=1}^{k}\frac{f_r(\Phi, s)}{s^{rp+1}}, \quad r = 1, 2, 3, 4\cdots. \tag{4.53}$$

Residual Mohand function is given by:

$$\mathcal{M}_{\Omega}Res(\Phi, s) = \Psi(\Phi, s) - \frac{\cos(\Phi)}{s} - \frac{a}{s^p}\Big[\frac{\partial^2\Psi(\Phi, s)}{\partial\Phi^2}\Big] + \frac{1}{s^p}\Big[\frac{\partial\Psi(\Phi, s)}{\partial\Phi}\Big] = 0, \tag{4.54}$$

and the k^{th}-MRFs as:

$$\mathcal{M}_{\Omega}Res_k(\Phi, s) = \Psi_k(\Phi, s) - \frac{\cos(\Phi)}{s} - \frac{a}{s^p}\Big[\frac{\partial^2\Psi_k(\Phi, s)}{\partial\Phi^2}\Big] + \frac{1}{s^p}\Big[\frac{\partial\Psi_k(\Phi, s)}{\partial\Phi}\Big] = 0. \tag{4.55}$$

The following procedures should be implemented to determine the value of $f_r(\Phi, s)$ for $r = 1, 2, 3, ...$: replace the r^{th}-Mohand residual function Eq 4.55 for the r^{th}-truncated series Eq 4.53, and multiply

the expression by s^{rp+1} for solving the relation, $\lim_{s\to\infty}(s^{rp+1})M_{\Omega}Res_{\Psi,r}(\Phi, s)) = 0$ for $r = 1, 2, 3, \cdots$. Some terms that we obtain are as follows:

$$f_1(\Phi, s) = \sin(\Phi) - a\cos(\Phi), \tag{4.56}$$

$$f_2(\Phi, s) = \left(a^2 - 1\right)\cos(\Phi) - 2a\sin(\Phi), \tag{4.57}$$

$$f_3(\Phi, s) = \left(3a^2 - 1\right)\sin(\Phi) - a\left(a^2 - 3\right)\cos(\Phi), \tag{4.58}$$

$$f_4(\Phi, s) = \left(a^4 - 6a^2 + 1\right)\cos(\Phi) - 4a\left(a^2 - 1\right)\sin(\Phi), \tag{4.59}$$

and so on.
To obtain the desired result, the function $f_r(\Phi, s)$ should be substituted into Eq 4.53.

$$\Psi(\Phi, s) = \frac{\cos(\Phi)}{s} + \frac{\sin(\Phi) - a\cos(\Phi)}{s^{p+1}} + \frac{\left(a^2 - 1\right)\cos(\Phi) - 2a\sin(\Phi)}{s^{2p+1}} + \frac{\left(3a^2 - 1\right)\sin(\Phi) - a\left(a^2 - 3\right)\cos(\Phi)}{s^{3p+1}} + \frac{\left(a^4 - 6a^2 + 1\right)\cos(\Phi) - 4a\left(a^2 - 1\right)\sin(\Phi)}{s^{4p+1}} + \cdots. \tag{4.60}$$

Apply the inverse operator of MT to obtain the final solution:

$$\Psi(\Phi, \Omega) = \cos(\Phi) + \frac{\Omega^p(\sin(\Phi) - a\cos(\Phi))}{\Gamma(p+1)} + \frac{\Omega^{2p}\left(\left(a^2 - 1\right)\cos(\Phi) - 2a\sin(\Phi)\right)}{\Gamma(2p+1)} + \frac{\Omega^{4p}\left(\left(a^4 - 6a^2 + 1\right)\cos(\Phi) - 4a\left(a^2 - 1\right)\sin(\Phi)\right)}{\Gamma(4p+1)}\frac{\Omega^{3p}\left(a\left(\left(a^2 - 3\right)\cos(\Phi) - 3a\sin(\Phi)\right) + \sin(\Phi)\right)}{\Gamma(3p+1)} + \cdots. \tag{4.61}$$

4.6. Problem 3 solution using MTIM

Suppose the following time FADE:

$$D^p_{\Omega}\Psi(\Phi, \Omega) = a\frac{\partial^2\Psi(\Phi, \Omega)}{\partial\Phi^2} - \frac{\partial\Psi(\Phi, \Omega)}{\partial\Phi}, \text{ where } 0 < p \leq 1. \tag{4.62}$$

Initial condition

$$\Psi(\Phi, 0) = \cos(\Phi). \tag{4.63}$$

Apply the MT on Eq 4.62:

$$M[D^p_{\Omega}\Psi(\Phi, \Omega)] = \frac{1}{s^p}\Big(\sum_{k=0}^{m-1}\frac{\Psi^{(k)}(\Phi, 0)}{s^{2-p+k}} + M\Big[a\frac{\partial^2\Psi(\Phi, \Omega)}{\partial\Phi^2} - \frac{\partial\Psi(\Phi, \Omega)}{\partial\Phi}\Big)\Big]\Big). \tag{4.64}$$

Apply the inverse operator of MT on Eq 4.64:

$$\Psi(\Phi, \Omega) = M^{-1}\Big[\frac{1}{s^p}\Big(\sum_{k=0}^{m-1}\frac{\Psi^{(k)}(\Phi, \eta, 0)}{s^{2-p+k}} + M\Big[a\frac{\partial^2\Psi(\Phi, \Omega)}{\partial\Phi^2} - \frac{\partial\Psi(\Phi, \Omega)}{\partial\Phi}\Big]\Big)\Big]. \tag{4.65}$$

Iteratively utilize the MT to get the following result:

$$\begin{aligned}\Psi_0(\Phi,\Omega) &= M^{-1}\Big[\frac{1}{s^p}\Big(\sum_{k=0}^{m-1}\frac{\Psi^{(k)}(\Phi,0)}{s^{2-p+k}}\Big)\Big]\\ &= M^{-1}\Big[\frac{\Psi(\Phi,0)}{s^2}\Big]\\ &= \cos(\Phi).\end{aligned}$$

Eq 4.62 is solved using the R-L integral to get:

$$\Psi(\Phi,\Omega) = \cos(\Phi) + M\Big[a\frac{\partial^2\Psi(\Phi,\Omega)}{\partial\Phi^2} - \frac{\partial\Psi(\Phi,\Omega)}{\partial\Phi}\Big]. \tag{4.66}$$

Some of the terms that the MITM method produces are as follows:

$$\Psi_0(\Phi,\Omega) = \cos(\Phi), \tag{4.67}$$

$$\Psi_1(\Phi,\Omega) = \frac{\Omega^p(\sin(\Phi) - a\cos(\Phi))}{\Gamma(p+1)}, \tag{4.68}$$

$$\Psi_2(\Phi,\Omega) = \frac{\Omega^{2p}\Big(\Big(a^2-1\Big)\cos(\Phi) - 2a\sin(\Phi)\Big)}{\Gamma(2p+1)}, \tag{4.69}$$

$$\Psi_3(\Phi,\Omega) = -\frac{\Omega^{3p}\Big(a\Big(\Big(a^2-3\Big)\cos(\Phi) - 3a\sin(\Phi)\Big) + \sin(\Phi)\Big)}{\Gamma(3p+1)}, \tag{4.70}$$

$$\Psi_4(\Phi,\Omega) = \frac{\Omega^{4p}\Big(\Big(a^4-6a^2+1\Big)\cos(\Phi) - 4a\Big(a^2-1\Big)\sin(\Phi)\Big)}{\Gamma(4p+1)}. \tag{4.71}$$

The final solution is:

$$\Psi(\Phi,\Omega) = \Psi_0(\Phi,\Omega) + \Psi_1(\Phi,\Omega) + \Psi_2(\Phi,\Omega) + \Psi_3(\Phi,\Omega) + \Psi_4(\Phi,\Omega) + \cdots, \tag{4.72}$$

$$\begin{aligned}\Psi(\Phi,\Omega) = \cos(\Phi) &+ \frac{\Omega^p(\sin(\Phi) - a\cos(\Phi))}{\Gamma(p+1)} + \frac{\Omega^{2p}\Big(\Big(a^2-1\Big)\cos(\Phi) - 2a\sin(\Phi)\Big)}{\Gamma(2p+1)}\\ &- \frac{\Omega^{3p}\Big(a\Big(\Big(a^2-3\Big)\cos(\Phi) - 3a\sin(\Phi)\Big) + \sin(\Phi)\Big)}{\Gamma(3p+1)} + \frac{\Omega^{4p}\Big(\Big(a^4-6a^2+1\Big)\cos(\Phi) - 4a\Big(a^2-1\Big)\sin(\Phi)\Big)}{\Gamma(4p+1)} + \cdots.\end{aligned} \tag{4.73}$$

Figure 12, graphical representation of approximate solution for different values of p of $\Psi(\Phi,\Omega)$ for $\Omega = 0.1$. Figure 13, graphical representation of approximate solution for different values of p of $\Psi(\Phi,\Omega)$ for $\Omega = 0.1$. Figure 14, comparison of approximate solution for different values of p of $\Psi(\Phi,\Omega)$ for $\Omega = 0.1$. Figure 15, (a) MRPSM solution and (b) MTIM solution of $\Psi(\Phi,\Omega)$ for $p = 1$ and $\Omega = 0.1$. Figure 16, (a) MRPSM solution and (b) MTIM solution comparison of $\Psi(\Phi,\Omega)$ for $p = 1$ and $\Omega = 0.1$. Table 5, the approximate solution comparison for the fractional order p of $\Psi(\Phi,\Omega)$ for $\Omega = 0.1$ of problem 3. Table 6, the approximate solution comparison for the fractional order p of $\Psi(\Phi,\Omega)$ for $\Omega = 0.1$ of problem 3.

In summary, the graphical results in Figures 12 to 16 further confirm the accuracy and effectiveness of the MRPSM and MTIM methods in solving FADEs. Both methods provide consistent and reliable solutions, and the visualizations of the solutions in both 2D and 3D formats offer valuable insights into the behavior of fractional-order systems. These results demonstrate the power of the proposed methods in solving complex fractional-order differential equations.

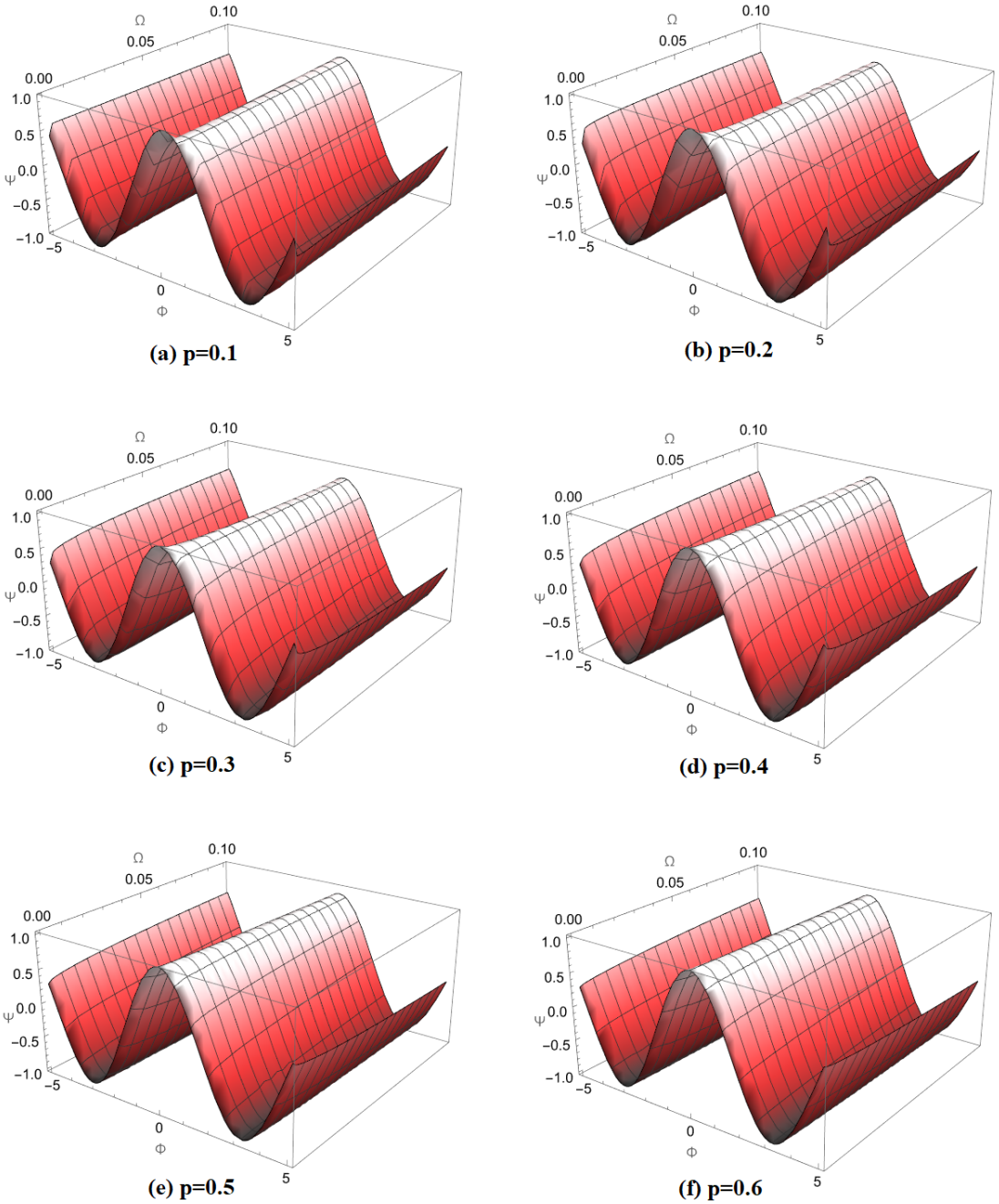

Figure 12. Graphical representation of approximate solution for different values of p of $\Psi(\Phi, \Omega)$ for $\Omega = 0.1$.

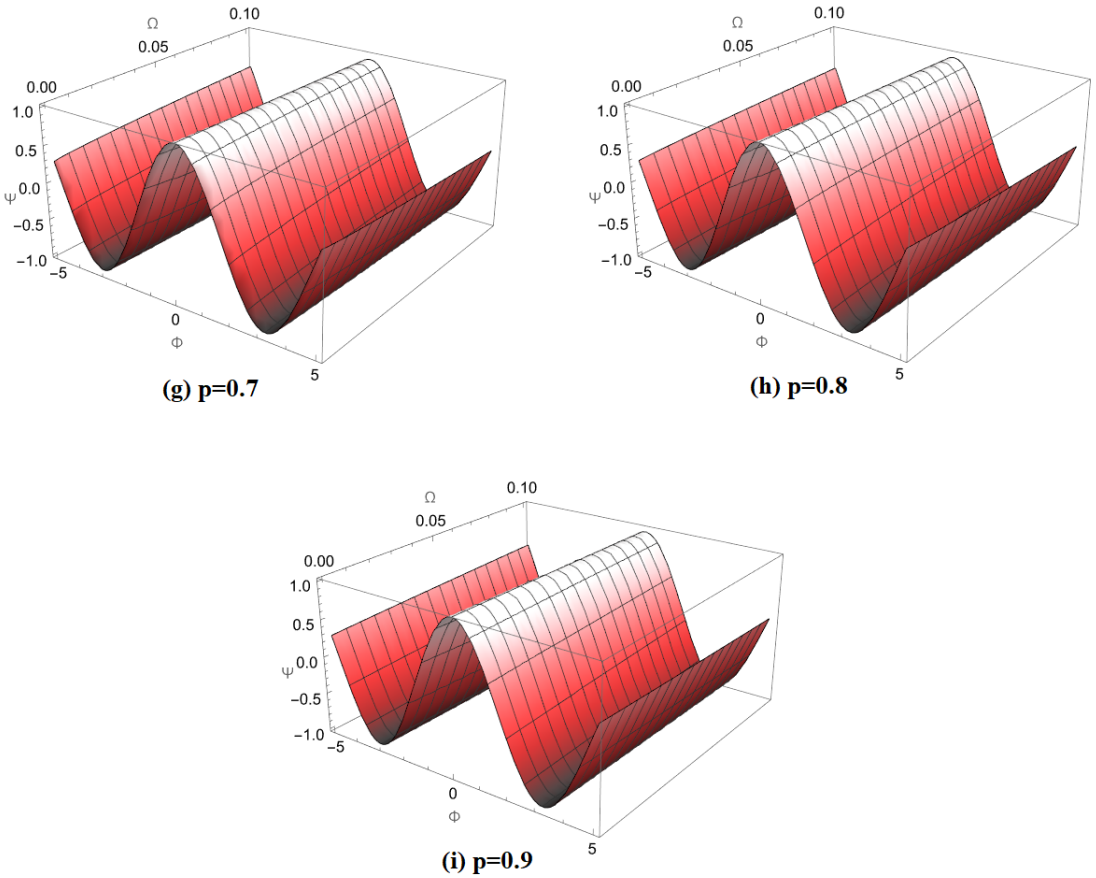

Figure 13. Graphical representation of approximate solution for different values of p of $\Psi(\Phi, \Omega)$ for $\Omega = 0.1$.

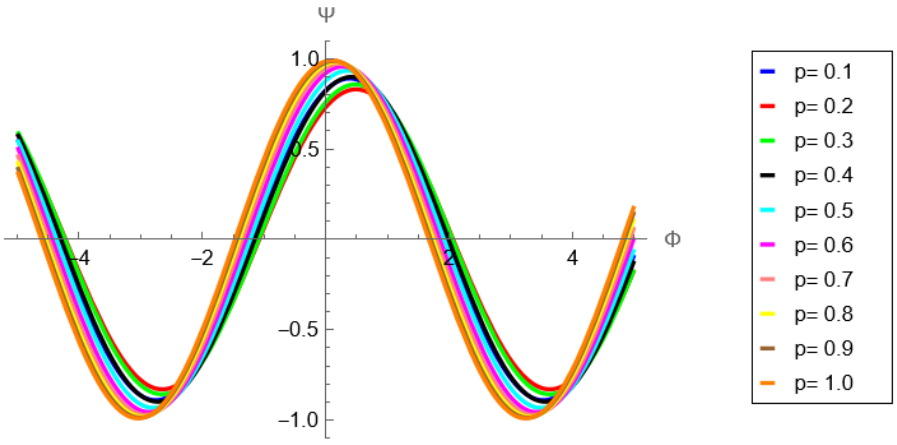

Figure 14. Comparison of approximate solution for different values of p of $\Psi(\Phi, \Omega)$ for $\Omega = 0.1$.

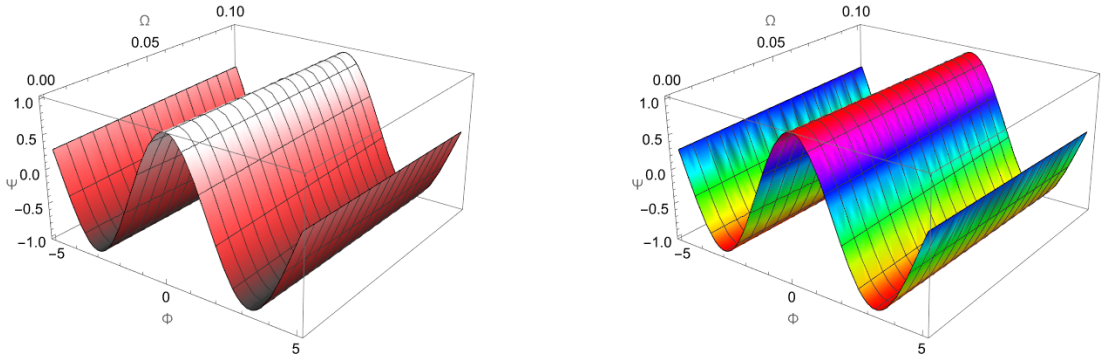

(a) MRPSM Solution **(b) MTIM Solution**

Figure 15. (a) MRPSM solution and (b) MTIM solution of $\Psi(\Phi, \Omega)$ for $p = 1$ and $\Omega = 0.1$.

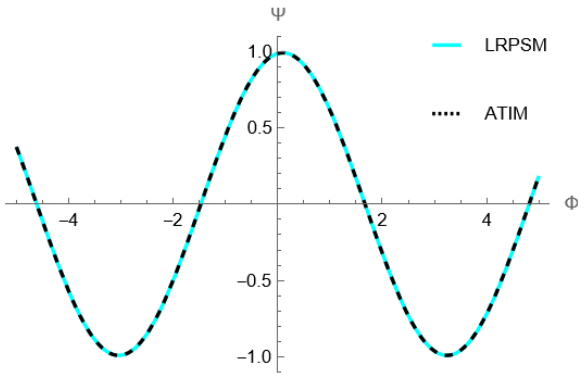

Figure 16. (a) MRPSM solution and (b) MTIM solution comparison of $\Psi(\Phi, \Omega)$ for $p = 1$ and $\Omega = 0.1$.

Table 5. The approximate solution comparison for the fractional order p of $\Psi(\Phi, \Omega)$ for $\Omega = 0.1$ of problem 3.

Φ	$MRPSM_{p=0.1}$	$MRPSM_{p=0.2}$	$MRPSM_{p=0.3}$	$MRPSM_{p=0.4}$	$MRPSM_{p=0.5}$	$MTIM_{p=0.5}$
1	0.7263668	0.7249992	0.7448338	0.7512493	0.7395935	0.7395935
2	-0.0400597	0.0523319	0.0460541	-0.0085039	-0.0779225	-0.0779225
3	-0.7696556	-0.6684490	-0.6950675	-0.7604387	-0.8237969	-0.8237969
4	-0.7916336	-0.7746611	-0.7971473	-0.8132296	-0.8122762	-0.8122762
5	-0.0857873	-0.1686533	-0.1663335	-0.1183409	-0.0539524	-0.0539524
6	0.6989314	0.5924135	0.6174065	0.6853498	0.7539749	0.7539749
7	0.8410559	0.8088181	0.8335058	0.8589331	0.8687013	0.8687013
8	0.2099174	0.2815990	0.2832837	0.2428172	0.1847476	0.1847476
9	-0.6142181	-0.5045209	-0.5273881	-0.5965436	-0.6690621	-0.6690621
10	-0.8736444	-0.8267866	-0.8531818	-0.8874451	-0.9077392	-0.9077392

Table 6. The approximate solution comparison for the fractional order p of $\Psi(\Phi, \Omega)$ for $\Omega = 0.1$ of problem 3.

Φ	$MRPSM_{p=0.6}$	$MRPSM_{p=0.7}$	$MRPSM_{p=0.8}$	$MRPSM_{p=0.9}$	$MRPSM_{p=1.0}$	$MTIM_{p=1.0}$
1	0.7163360	0.6885956	0.6611363	0.6364310	0.6154248	0.6154248
2	-0.1452003	-0.2036107	-0.2516376	-0.2899815	-0.3200728	-0.3200728
3	-0.8732402	-0.9086184	-0.9330571	-0.9497864	-0.9612970	-0.9612970
4	-0.7984270	-0.7782464	-0.7566282	-0.7363620	-0.7187091	-0.7187091
5	0.0104562	0.0676417	0.1154411	0.1540702	0.1846566	0.1846566
6	0.8097261	0.8513404	0.8813745	0.9028510	0.9182499	0.9182499
7	0.8645375	0.8523206	0.8369761	0.8215547	0.8076084	0.8076084
8	0.1244970	0.0696812	0.0230658	-0.0150751	-0.0455444	-0.0455444
9	-0.7300053	-0.7770228	-0.8120511	-0.8378450	-0.8568240	-0.8568240
10	-0.9133442	-0.9093356	-0.9005720	-0.8903040	-0.8803435	-0.8803435

5. Conclusions

In this study, we have effectively applied the MTIM and the MRPSM to solve the nonlinear FADEs. By incorporating the Caputo operator, we have enhanced the modeling of systems characterized by complex behaviors, improving the understanding of fractional-order differential equations. Our results demonstrate that both MTIM and MRPSM provide accurate approximate solutions that closely align with the exact ones, as shown by the accompanying tables and figures. These methods offer a robust framework for investigating the nonlinear behaviors of fractional systems, which are prevalent in physical sciences, engineering, and other fields. The inclusion of fractional derivatives defined by the Caputo operator introduces an added layer of complexity, enabling a more precise representation of nonlocal behaviors in the systems studied. The graphical analyses further confirm the utility of these methods in computational physics, where precise and efficient solutions are invaluable. Overall, this work contributes to advancing the field of fractional calculus, offering novel techniques for scholars working with nonlinear systems. The approaches presented here lay the groundwork for future research and exploration in this area.

Author contributions

A.S.A: Conceptualization, Visualization, Funding, Data curation, Resources, Writing-review & editing; H. Y.: Formal analysis, Project administration, Data curation, validation; A. M. M.: Investigation, Validation, Resources, Software. All authors have read and agreed to the published version of the manuscript.

Funding

Princess Nourah bint Abdulrahman University Researchers Supporting Project number (PNURSP2025R183), Princess Nourah bint Abdulrahman University, Riyadh, Saudi Arabia. This work was supported by the Deanship of Scientific Research, Vice Presidency for Graduate Studies and

Scientific Research, King Faisal University, Saudi Arabia (GrantKFU242968).

Conflict of interest

The authors declare that they have no conflict of interest.

Acknowledgments

Princess Nourah bint Abdulrahman University Researchers Supporting Project number (PNURSP2025R183), Princess Nourah bint Abdulrahman University, Riyadh, Saudi Arabia. This work was supported by the Deanship of Scientific Research, Vice Presidency for Graduate Studies and Scientific Research, King Faisal University, Saudi Arabia (GrantKFU242968).

Use of Generative-AI tools declaration

The authors declare they have not used Artificial Intelligence (AI) tools in the creation of this article.

References

1. J. Gray, Change and variations: A history of differential equations to 1900, New York, NY, USA: (2021) Springer. https://doi.org/10.1007/978-3-030-70575-6
2. H. T. Davis, Introduction to nonlinear differential and integral equations. US Atomic Energy Commission, 1960.
3. X. Zheng, J. Jia, X. Guo, Eliminating solution singularity of variably distributed-order time-fractional diffusion equation via strongly singular initial distribution, *Chaos, Soliton. Fract.*, **174** (2023), 113908. https://doi.org/10.1007/978-3-030-70575-6
4. X. H. Zhao, Multi-solitons and integrability for a (2+1)-dimensional variable coefficients Date-Jimbo-Kashiwara-Miwa equation, *Appl. Math. Lett.*, **149** (2024), 108895. https://doi.org/10.1016/j.aml.2023.108895
5. Z. Z. Lan, Semirational rogue waves of the three coupled higher-order nonlinear Schrodinger equations, *Appl. Math. Lett.*, **147** (2024), 108845. https://doi.org/10.1016/j.aml.2023.108845
6. Y. Kai, Z. Yin, On the Gaussian traveling wave solution to a special kind of Schrodinger equation with logarithmic nonlinearity, *Mod. Phys. Lett. B*, **36** (2021), 2150543. https://doi.org/10.1142/S0217984921505436
7. J. Xie, Z. Xie, H. Xu, Z. Li, W. Shi, J. Ren, et al., Resonance and attraction domain analysis of asymmetric duffing systems with fractional damping in two degrees of freedom, *Chaos, Soliton. Fract.*, **187** (2024), 115440. https://doi.org/10.1016/j.chaos.2024.115440
8. C. Zhu, S. A. Idris, M. E. M. Abdalla, S. Rezapour, S. Shateyi, B. Gunay, Analytical study of nonlinear models using a modified Schrodinger's equation and logarithmic transformation, *Results Phys.*, **55** (2023), 107183. https://doi.org/10.1016/j.rinp.2023.107183

9. G. Shuangjian, D. Apurba, Cohomology and deformations of generalized reynolds operators on leibniz algebras, *Rocky Mt. J. Math.*, **54** (2024), 161–178. https://doi.org/10.1216/rmj.2024.54.161
10. T. A. A. Ali, Z. Xiao, H. Jiang, B. Li, A class of digital integrators based on trigonometric quadrature rules, *IEEE T. Ind. Electron.*, **71** (2024), 6128–6138. https://doi.org/10.1109/TIE.2023.3290247
11. Z. Z. Lan, Multi-soliton solutions, breather-like and bound-state solitons for complex modified Korteweg-de Vries equation in optical fibers, *Chinese Phys. B*, **33** (2024), 060201. https://doi.org/10.1088/1674-1056/ad39d7
12. Z. Z. Lan, N-soliton solutions, Backlund transformation and Lax Pair for a generalized variable-coefficient cylindrical Kadomtsev-Petviashvili equation, *Appl. Math. Lett.*, **158** (2024), 109239. https://doi.org/10.1016/j.aml.2024.109239
13. Z. Z. Lan, Multiple Soliton Asymptotics in a Spin-1 Bose-Einstein Condensate, *Chinese Phys. Lett.*, **41** (2024), 090501. https://doi.org/10.1088/0256-307X/41/9/090501
14. M. Z. Liu, D. Li, Properties of analytic solution and numerical solution of multi-pantograph equation, *Appl. Math. Comput.*, **155** (2004), 853–871. https://doi.org/10.1016/j.amc.2003.07.017
15. A. El-Ajou, Z. Odibat, S. Momani, A. Alawneh, Construction of analytical solutions to fractional differential equations using homotopy analysis method, *IAENG Int. J. Appl. Math.*, **40** (2010).
16. Y. F. Luchko, H. M. Srivastava, The exact solution of certain differential equations of fractional order by using operational calculus, *Comput. Math. Appl.*, **29** (1995), 73–85. https://doi.org/10.1016/0898-1221(95)00031-S
17. A. Saadatmandi, M. Dehghan, A new operational matrix for solving fractional-order differential equations, *Comput. Math. Appl.*, **59** (2010), 1326–1336. https://doi.org/10.1016/j.camwa.2009.07.006
18. A. M. Wazwaz, The modified decomposition method for analytic treatment of differential equations, *Appl. Math. Comput.*, **173** (2006), 165–176. https://doi.org/10.1016/j.amc.2005.02.048
19. A. El-Ajou, O. A. Arqub, S. Momani, Approximate analytical solution of the nonlinear fractional KdV-Burgers equation: A new iterative algorithm, *J. Comput. Phys.*, **293** (2015), 81–95. https://doi.org/10.1016/j.jcp.2014.08.004
20. S. Das, Analytical solution of a fractional diffusion equation by variational iteration method, *Comput. Math. Appl.*, **57** (2009), 483–487. https://doi.org/10.1016/j.camwa.2008.09.045
21. S. Alshammari, M. M. Al-Sawalha, R. Shah, Approximate analytical methods for a fractional-order nonlinear system of Jaulent-Miodek equation with energy-dependent Schrodinger potential, *Fractal Fract.*, **7** (2023), 140. https://doi.org/10.3390/fractalfract7020140
22. Y. Qin, A. Khan, I. Ali, M. Al Qurashi, H. Khan, D. Baleanu, An efficient analytical approach for the solution of certain fractional-order dynamical systems. *Energies*, **13** (2020), 2725. https://doi.org/10.3390/en13112725
23. A. A. Alderremy, N. Iqbal, S. Aly, K. Nonlaopon, Fractional series solution construction for nonlinear fractional reaction-diffusion Brusselator model utilizing Laplace residual power series, *Symmetry*, **14** (2022), 1944. https://doi.org/10.3390/sym14091944

24. M. M. Al-Sawalha, A. Khan, O. Y. Ababneh, T. Botmart, Fractional view analysis of Kersten-Krasil'shchik coupled KdV-mKdV systems with non-singular kernel derivatives, *AIMS Math.*, **7** (2022), 18334–18359. https://doi.org/10.3934/math.20221010
25. H. Yasmin, A. S. Alshehry, A. H. Ganie, A. M. Mahnashi, Perturbed Gerdjikov-Ivanov equation: Soliton solutions via Backlund transformation, *Optik*, **298** (2024), 171576. https://doi.org/10.1016/j.ijleo.2023.171576
26. A. U. K. Niazi, N. Iqbal, F. Wannalookkhee, K. Nonlaopon, Controllability for fuzzy fractional evolution equations in credibility space, *Fractal Fract.*, **5** (2021), 112. https://doi.org/10.3390/fractalfract5030112
27. E. M. Elsayed, K. Nonlaopon, The analysis of the fractional-order Navier-Stokes equations by a novel approach, *J. Funct. Space.*, **2022** (2022), 8979447. https://doi.org/10.1155/2022/8979447
28. M. Naeem, H. Rezazadeh, A. A. Khammash, S. Zaland, Analysis of the fuzzy fractional-order solitary wave solutions for the KdV equation in the sense of Caputo-Fabrizio derivative, *J. Math.*, **2022** (2022), 3688916. https://doi.org/10.1155/2022/3688916
29. M. Alqhtani, K. M. Saad, R. Shah, W. M. Hamanah, Discovering novel soliton solutions for (3+1)-modified fractional Zakharov-Kuznetsov equation in electrical engineering through an analytical approach, *Opt. Quant. Electron.*, **55** (2023), 1149. https://doi.org/10.1007/s11082-023-05407-2
30. S. Meng, F. Meng, F. Zhang, Q. Li, Y. Zhang, A. Zemouche, Observer design method for nonlinear generalized systems with nonlinear algebraic constraints with applications, *Automatica*, **162** (2024), 111512. https://doi.org/10.1016/j.automatica.2024.111512
31. F. Meng, A. Pang, X. Dong, C. Han, X. Sha, H-∞ optimal performance design of an unstable plant under bode integral constraint, *Complexity*, **2018** (2018), 4942906. https://doi.org/10.1155/2018/4942906
32. F. Meng, D. Wang, P. Yang, G. Xie, Application of sum of squares method in nonlinear H-∞ control for satellite attitude maneuvers, *Complexity*, **2019** (2019), 5124108. https://doi.org/10.1155/2019/5124108
33. S. Liang, Y. Gao, C. Hu, A. Hao, H. Qin, Efficient photon beam diffusion for directional subsurface scattering, *IEEE T. Vis. Comput. Gr.*, (2024). https://doi.org/10.1109/TVCG.2024.3447668
34. J. Wang, J. Ji, Z. Jiang, L. Sun, Traffic flow prediction based on spatiotemporal potential energy fields, *IEEE T. Knowl. Data En.*, **35** (2022), 9073–9087. https://doi.org/10.1109/TKDE.2022.3221183
35. T. Zhang, S. Xu, W. Zhang, New approach to feedback stabilization of linear discrete time-varying stochastic systems, *IEEE T. Automat. Contr.*, (2024). https://doi.org/10.1109/TAC.2024.3482119
36. B. O. R. I. S. Baeumer, D. A. Benson, M. M. Meerschaert, Advection and dispersion in time and space, *Physica A*, **350** (2005), 245–262. https://doi.org/10.1016/j.physa.2004.11.008
37. S. Momani, Z. Odibat, Numerical solutions of the space-time fractional advection-dispersion equation, *Numer. Meth. Part. D. E.*, **24** (2008), 1416–1429. https://doi.org/10.1002/num.20324
38. O. A. Arqub, Series solution of fuzzy differential equations under strongly generalized differentiability, *J. Adv. Res. Appl. Math.*, **5** (2013), 31–52. https://doi.org/10.5373/jaram.1447.051912

39. O. A. Arqub, A. El-Ajou, Z. A. Zhour, S. Momani, Multiple solutions of nonlinear boundary value problems of fractional order: A new analytic iterative technique, *Entropy*, **16** (2014), 471–493. https://doi.org/10.3390/e16010471
40. A. El-Ajou, O. A. Arqub, S. Momani, Approximate analytical solution of the nonlinear fractional KdV-Burgers equation: A new iterative algorithm, *J. Comput. Phys.*, **293** (2015), 81–95. https://doi.org/10.1016/j.jcp.2014.08.004
41. F. Xu, Y. Gao, X. Yang, H. Zhang, Construction of fractional power series solutions to fractional Boussinesq equations using residual power series method, *Math. Probl. Eng.*, **2016** (2016). https://doi.org/10.1155/2016/5492535
42. J. Zhang, Z. Wei, L. Li, C. Zhou, Least-squares residual power series method for the time-fractional differential equations, *Complexity*, **2019** (2019), 1–15. https://doi.org/10.1155/2019/6159024
43. I. Jaradat, M. Alquran, R. Abdel-Muhsen, An analytical framework of 2D diffusion, wave-like, telegraph, and Burgers' models with twofold Caputo derivatives ordering, *Nonlinear Dynam.*, **93** (2018), 1911–1922. https://doi.org/10.1007/s11071-018-4297-8
44. I. Jaradat, M. Alquran, K. Al-Khaled, An analytical study of physical models with inherited temporal and spatial memory, *Eur. Phys. J. Plus*, **133** (2018), 1–11. https://doi.org/10.1140/epjp/i2018-12007-1
45. M. Alquran, K. Al-Khaled, S. Sivasundaram, H. M. Jaradat, Mathematical and numerical study of existence of bifurcations of the generalized fractional Burgers-Huxley equation, *Nonlinear Stud.*, **24** (2017), 235–244.
46. M. Alquran, M. Ali, M. Alsukhour, I. Jaradat, Promoted residual power series technique with Laplace transform to solve some time-fractional problems arising in physics, *Results Phys.*, **19** (2020), 103667. https://doi.org/10.1016/j.rinp.2020.103667
47. T. Eriqat, A. El-Ajou, N. O. Moa'ath, Z. Al-Zhour, S. Momani, A new attractive analytic approach for solutions of linear and nonlinear neutral fractional pantograph equations, *Chaos, Soliton. Fract.*, **138** (2020), 109957. https://doi.org/10.1016/j.chaos.2020.109957
48. M. Alquran, M. Alsukhour, M. Ali, I. Jaradat, Combination of Laplace transform and residual power series techniques to solve autonomous n-dimensional fractional nonlinear systems, *Nonlinear Eng.*, **10** (2021), 282–292. https://doi.org/10.1515/nleng-2021-0022
49. M. Mohand, A. Mahgoub, The new integral transform "Mohand Transform", *Adv. Theor. Appl. Math.*, **12** (2017), 113–120.
50. M. Nadeem, J. H. He, A. Islam, The homotopy perturbation method for fractional differential equations: Part 1 Mohand transform, *Int. J. Numer. Meth. H.*, **31** (2021), 3490–3504. https://doi.org/10.1108/HFF-11-2020-0703